Surface Modification for Promoting Durable, Efficient, and Selective Electrocatalysts

Quentin Lenne, Yann R. Leroux, Corinne Lagrost

Surface modification for promoting durable, efficient and selective electrocatalysts.

Quentin Lenne[a], Yann R. Leroux [a] and Corinne Lagrost*[a]

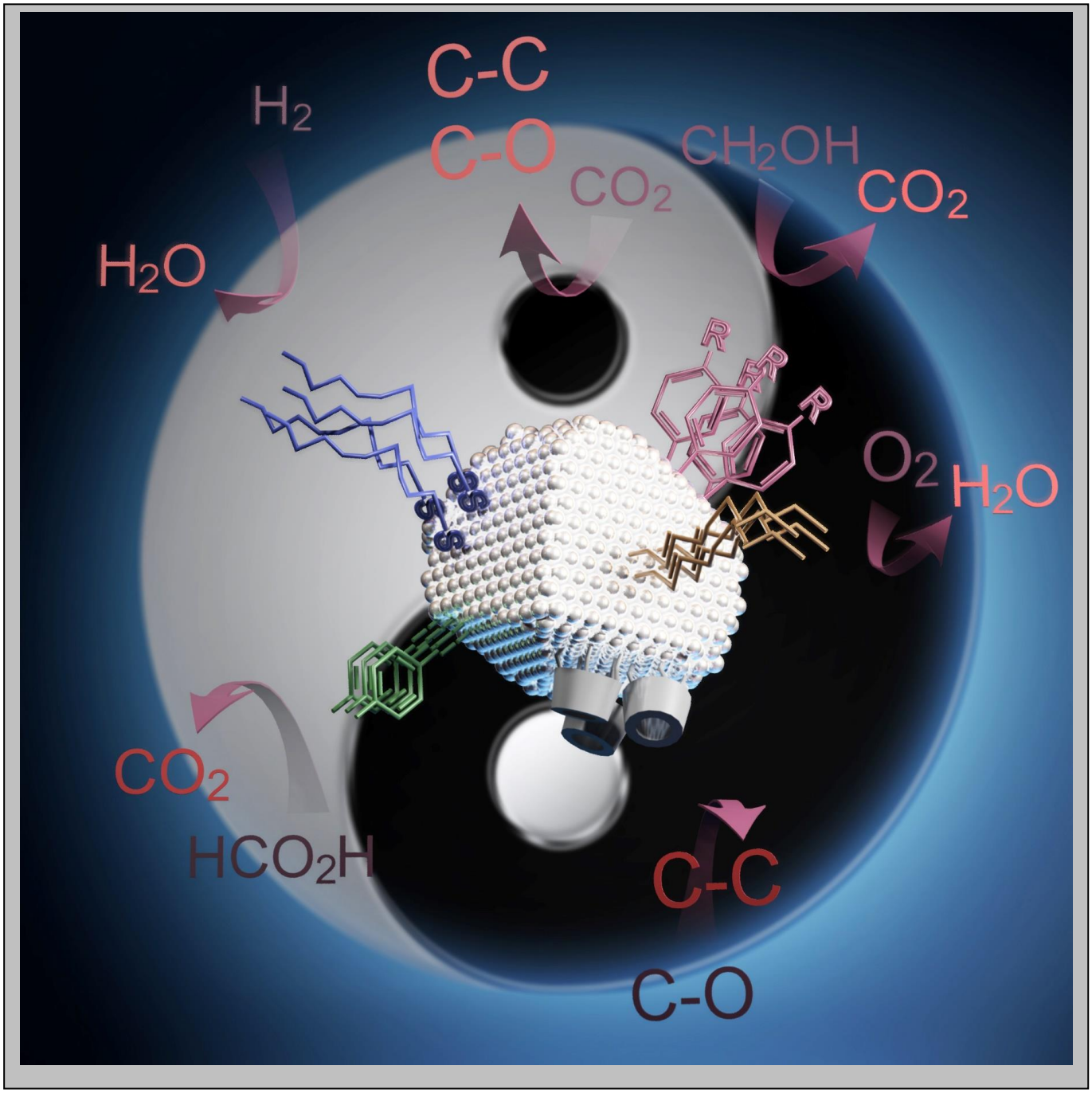

[a] M. Q. Lenne, Dr. Y.R. Leroux, Dr. C. Lagrost
ISCR-UMR 6226
CNRS and Univ Rennes
Campus de Beaulieu, F-35042 Rennes, France
E-mail: Corinne.lagrost@univ-rennes1.fr

Abstract: Intensive researches for the design of catalysts involved in energy conversion and fuel cell technologies have allowed great progress in field. However, durable, efficient and selective electrocatalytic systems for the activation of fuel molecules at the lowest cost are still needed. The most developed strategies consist in the tailoring of shape, size and composition of metallic nanomaterials. Yet deliberate surface modification of the catalysts should be considered as a promising alternative approach. The functionalization of metallic catalysts with organic ligands has been recently demonstrated to promote high catalytic activity. This review focus on the functionalization of metallic or alloy catalysts with organic ligands, showing the impact of the surface modification for different materials and different reactions. Hybrid systems based on this alternative strategy could contribute to the elaboration of cutting-edge systems for electrocatalysis.

1. Introduction.

1.1. Designing efficient, selective and durable catalysts?

Due to great stability, metal-based heterogeneous catalysts are the most popular systems in fuel molecules activation, including oxygen reduction reaction (ORR), carbon dioxide or monoxide reduction reaction (CO_2RR or CORR), hydrogen evolution reaction (HER), water oxidation, dihydrogen oxidation (HOR), methanol oxidation (MOR), formic acid oxidation (FAOR) and ethanol oxidation (EOR).

The nanostructuring of noble and non-noble metals with the manipulation of particle shape/size or the engineering of topmost layers with sub-monolayer of foreign metals is the subject of ongoing research. These strategies allow great progress in the field and have been extensively reviewed, e.g.[1-9] to quote a few. Interestingly, there are some similarities regarding the nature of the metal materials that are the most suitable for ORR, CORR, CO_2RR, COR, MOR, FAOR and HOR. Although some of these metal-based electrocatalysts exhibit high catalytic performance, most of the materials still face with large overpotential, low faradic efficiency and above all, a poor product selectivity. Actually, regarding the reactions considered in this review, which are multi-electrons multi-protons processes, the selectivity is very often linked to the control of site protonation or deprotonation which is quite difficult to reach with metallic catalysts. In contrast, molecular catalysts based on transition metal complexes offer the possibility to tune the chemical nature of the ligands associated to the metal center in order to decipher chemical (e.g. nucleophilic) attack on the activated substrates.[10,11] Thus, the presence of organic ligands allows a better control of selectivity. At this stage, we must outline that exploitation of the interaction between metal center and ligand is a widely implemented strategy in homogenous catalysis. However, the deliberate chemical functionalization of metallic electrocatalysts with organic ligands is much less explored than nanostructuring or use of molecular catalysts (being immobilized at a support or not). Traditionally, organic ligands or capping agents have been exploited for controlling the size and shape of metal-based nanoparticles, subsequently employed as electrocatalysts. They were usually considered as poisonous species, limiting the accessibility of catalytic sites, then deactivating the catalysts. Removal of the ligands is systematically considered for high performance and this step generally constitutes a very tedious task in the synthesis of nanocatalysts.

Nevertheless, the surface modification of metal-based electrocatalysts with organic linkers has recently emerged as a promising strategy for boosting the catalytic performances of metallic systems, notably nanostructures, bridging the gap between homogeneous and heterogeneous (electro-)catalysis.

1.2. Surface modification procedures.

There are numerous procedures for the immobilization of organic molecules to metallic surfaces including the chemisorption of monomers or polymers, the self-assembly, the covalent grafting and the electrostatic adsorption of charged molecules (e.g. citrate) or polymers (e.g. polyelectrolytes). These procedures result in the formation of monolayers, multilayers or polymer films. The monolayers allow well-organized layer structure with a possible fine molecular control of ligands orientation and spatial distribution. Polymers and multilayers, in spite of their usually disordered arrangement, generally exhibit higher surface coverage and apparent electrochemical stability. All these procedures generally lead to robust and durable attachment of organic molecules onto flat surfaces but also onto nanomaterials while the electrostatic adsorption corresponds to the weaker interaction between surface and ligands with binding energies usually lower than 85 $kJ.mol^{-1}$.[12]

Regarding the chemisorption and the self-assembly, the coordination ability of the organic ligand is related to its coordinately active chemical group (or atom) but also to the associated chemical substituent that could have an impact in terms of coordination strength and spatial requirement. Thiolates, phosphines, amines, carbenes, alkynyls are typical examples of binding moieties on coinage metals. Generally speaking, the binding strength follows the order thiolates ~ phosphines > alkynyls > amine according to Hard-Soft Acid-Base theory.[13] An important aspect lies in the orientation of the organic ligand with respect to the surface, which depends on the coordinately active groups. For instance, alkynyls can bind linearly to surface Au atoms through σ-bonds.

The reductive grafting of aryldiazonium salts is another strategy for the robust attachment of ligands onto surface. In contrast with other chemisorption procedures, this approach is not limited to metals and it can be applied to a wide range of materials including conducting (Au, Pt, Cu, Fe, Zn, stainless steel, Ni, carbon in all forms, etc), semi-conducting (Si, SiGe, Ge, GaAS, etc.), oxides (ITO, TiO_2, SnO_2, SiO_2, etc), and even insulating substrates (glass, PMMA, PET, PP, etc.).[14] Reduction of aryldiazonium cations produces very reactive aryl radicals that can bind metallic surfaces.[14] The covalent nature of the metal-carbon bond has been strongly suggested, although still disputed, with adsorption energies over 100 $kJ.mol^{-1}$ as predicted by theoretical calculations.[15] A direct evidence for the formation of Au-C covalent bonds on gold nanoparticles was provided through a Surface enhanced Raman scattering (SERS) study.[16] Especially, this method allows the preparation of extremely robust aryl-stabilized nanoparticles.[16-19]

1.3. Scope and organization of the review.

The scope of this review is to provide a comprehensive overview of the impact of deliberate chemical functionalization of catalysts with organic ligands on the electrocatalysis performance. We will consider key processes involved in sustainable energy conversion and fuel cells. We will mainly focus on ORR and CO_2RR along with a few examples involving HOR, MOR and FAOR. We will start first in section 2 with some basic generalities concerning ORR and CO_2RR including mechanistic pathways and activity on pure metals. MOR, FAOR and HOR will be also quickly discussed. The impact of modification of catalysts with organic ligands will be then reviewed considering single metals in section 3, from flat massive surfaces to nanomaterials, applied to CO_2RR, ORR and other oxidation processes (MOR, HOR, FAOR). Section 4 will be devoted to the chemical functionalization of alloys while in section 5 we will discuss the fundamentals of such molecular enhancement of electrocatalysis performance. A conclusion will finally summarize all the encountered effects.

Quentin Lenne received a BSc in chemistry from Univ. Rennes (France) in 2016. In 2018, he obtained a MSc in material sciences from Ludwig-Maximilians-Universität (München, Germany). He is currently pursuing his PhD at the Institut des Sciences Chimiques de Rennes, Univ. Rennes under the supervision of Dr. Corinne Lagrost and Dr. Yann Leroux. His research interests focus on nanomaterials and electrocatalysis, including hybrid nanoparticles, oxygen reduction reaction, carbon dioxide reduction reaction.

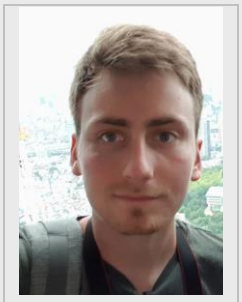

Yann Leroux received his PhD degree in 2007 from Paris Diderot University (France) where he focused his research on plasmonic devices and atomic contacts driven by electrochemistry. He gets interested in molecular electronics and organic chemistry during his postdoctoral position in Basel (Switzerland). Then, he joined the Institut des Sciences Chimiques de Rennes (France) where he is now a CNRS junior researcher. His research activity now focuses mainly on local electrochemistry and functionalization of electrode surfaces.

Corinne Lagrost is a CNRS Directrice de Recherche. She received her PhD degree in molecular electrochemistry from Paris Diderot University (France). After a post-doctoral stay in University of Amsterdam (The Netherlands), she obtained a CNRS permanent position at the Institut des Sciences Chimiques de Rennes, Univ. Rennes in 2001. Her research topics concern the electrochemical reactivity notably in unconventional media (ionic liquids, DES, etc), molecular functionalization of metallic surfaces and electrochemical properties.

2. Key electrocatalytic processes: generalities.

2.1. ORR.

Oxygen reduction reaction (ORR) is still a challenging reaction because of its slow rate and high overpotential. ORR in aqueous solutions is a highly irreversible process consisting in multiple coupled electron and proton transfers involving several oxygen-containing species.[4] The ORR mechanism includes many elementary steps, still widely discussed because of the complexity of the ORR kinetics.

Fundamentally, ORR on metal surfaces could either follow the direct 4 e^- pathway from O_2 to produce H_2O (R1 and R4) or the 2 e^- pathway (R2 and R5) that forms hydrogen peroxide (H_2O_2). H_2O_2 could be further converted into H_2O (R3 and R6), leading to an "indirect" 4 e^- pathway.

$O_2 + 4H^+ + 4e^- \rightarrow H_2O$ E° = 1.23 V vs RHE (R1)
$O_2 + 2H^+ + 2e^- \rightarrow H_2O_2$ E° = 0.70 V vs RHE (R2)
$H_2O_2 + 2H^+ + 2e^- \rightarrow 2H_2O$ E° = 1.76 V vs RHE (R3)

$O_2 + 2H_2O + 4e^- \rightarrow 4OH^-$ E° = 0.40 V vs RHE (R4)
$O_2 + H_2O + 2e^- \rightarrow HO_2^- + OH^-$ E° = -0.07 V vs RHE (R5)
$HO_2^- + H_2O + 2e^- \rightarrow 3OH^-$ E° = 0.87 V vs RHE (R6)
or $2\ HO_2^- \rightarrow 2\ OH^- + O_2$

These processes are clearly sensitive to the nature of catalysts' material and its structure but also to the pH, the presence of adsorbed species (electrolyte, intermediates) and the applied potential. Pt and Pt-based systems are the major ORR catalyst materials used under acidic conditions, allowing notably the direct 4 e^- pathway while gold, silver, mercury, and other non-noble metals (in alkaline solutions) were generally found to follow the 2e^- or "indirect" electrocatalytic pathways. However, gold nanomaterials, especially with exposed (100) facets,[20] as well as silver with facets in the order Ag(100) < Ag(111) < Ag(110),[21] show good performance for the conversion of O_2 into OH^- in alkaline media. Performances of catalysts following the 2e^- pathway are dependent on the reactivity of *OOH adsorbed intermediates. The 4e^- pathway involves up to three different adsorbed intermediates, which are strongly correlated, namely, *OOH, *O, *OH, depending on the associative or dissociative nature of the mechanism.[22,23] Both gold and silver nanomaterials are good catalysts for H_2O^- elimination catalysts, which may explain their better stability than Pt in long-term operations. They would accordingly be acceptable as catalysts for some applications, even considering their lower activity.[24] pH or spectator ions have significant impact on surface poisoning, which can dramatically decrease catalysts' performances. The pH variation greatly influences the adsorption of species, whether intermediates and/or counter ions. For instance, SO_4^{2-} that adsorbs strongly on Pt under acidic conditions does not significantly adsorb in strongly alkaline media under the typical working potential range (i.e. 0 < E < 1 V).[25]

To summarize, the maximum catalytic activity for ORR depends on a balance between adsorption energies of reactive intermediates and on the surface coverage of oxygenated spectators species or specifically adsorbed anions.

2.2 CO_2RR.

Generally performed in neutral media, the electrochemical reduction of carbon dioxide (CO_2RR) is a very demanding reaction due to the very stable nature of CO_2. It is widely accepted that the large overpotential needed for CO_2RR arises from the first step of the reaction: the CO_2 adsorbed at the surface is converted into the key intermediate adsorbed $CO_2^{\bullet-}$ which is believed to be the *rate-determining step* (Reaction (R14)).[26]

This multi-step reaction can take place via 2-, 4-, up to 12- e^- pathways (Reactions (R7)-(R12)).[27] Actually, the overpotentials needed for achieving these reductions are much more negative than the equilibrium ones due to necessity to first form $CO_2^{\bullet-}$ (R14):

$CO_2 + 2H^+ + 2e^- \rightarrow CO + H_2O$	E° = -0.52 V vs RHE	(R7)
$CO_2 + 2H^+ + 2e^- \rightarrow HCOOH$	E° = -0.61 V vs RHE	(R8)
$CO_2 + 4H^+ + 4e^- \rightarrow HCHO + H_2O$	E° = -0.51 V vs RHE	(R9)
$CO_2 + 6H^+ + 6e^- \rightarrow CH_3OH + H_2O$	E° = -0.38 V vs RHE	(R10)
$CO_2 + 8H^+ + 8e^- \rightarrow CH_4 + 2H_2O$	E° = -0.24 V vs RHE	(R11)
$CO_2 + 12H^+ + 12e^- \rightarrow C_2H_4 + 4H_2O$	E° = -0.34 V vs RHE	(R12)
$2H^+ + 2e^- \rightarrow H_2$	E° = -0.40 V vs RHE	(R13)
$CO_2 + e^- \rightarrow CO_2^{\bullet-}$	E° = -1.90 V vs RHE	(R14)

It is worth noting that the CO_2 reduction reactions takes place at reduction potentials thermodynamically comparable to that of the hydrogen evolution reaction (HER) (Reaction (R13), being then a competitive reaction. Surfaces showing high affinity for *H mostly end up by producing H_2 since its kinetics is much more facile and therefore inhibit the surface reactivity towards CO_2RR.

Due to the multiplicity of possible products, the main challenge remains in selectivity and not really in the overall activity.

The reactivity of $*CO_2^{\bullet-}$ with surfaces is the key parameter responsible for the final distribution of products as shown by Hori *et al*. who examined CO_2RR on diverse metals.[28] Roughly speaking, whether the oxygen atom or the carbon atom binds to the electrode surface will determine the following step, hence the selectivity.[29]

The first situation usually occurs on metals such as Sn, Pb, Hg, In, etc.[30-32] The $*CO_2^{\bullet-}$ intermediate is poorly bound, and its protonation generates *OCHO, leading to formic acid (HCOOH) but requires very large overpotentials. When the carbon atom of $*CO_2^{\bullet-}$ binds the surface (case for Au, Ag, Cu, Zn, Pt, Ni, Sn) a *COOH intermediate is produced leading to *CO, further forming CO or hydrocarbons/alcohols.[33,34] However, the further reduction of *CO to C_1 or C_2 compounds is only possible on Cu.[35] Actually, Cu is the only single-metal electrode that could produce C_2 feedstocks (hydrocarbons and oxygenates) with reasonable reactions rates and good faradaic efficiencies. The major bottlenecks are the low selectivity towards multi-carbon products and the competition with the hydrogen evolution reaction (HER).[36,37] Within C_1 and C_2 products we can distinguish the fully reduced ones (i.e. CH_4 and C_2H_4) and the partially reduced ones (i.e. CH_3OH). CH_4 is believed to be formed through the reduction of *COH by progressive protonation at rather important overpotential.[38,39] At lower overpotentials, the formation of C_2 products may involve coupling reactions between CHO* and CH_2O*.[33,40] Selectivity of Cu generally remains poor (at -1.44 V vs NHE, current density of 5 $mA.cm^{-2}$): along with ≈55% hydrocarbons (CH_4, C_2H_4), a proportion of formate (≈10%) and hydrogen (≈20%) are formed as well as alcohols (≈10%) but also acetone, ethanal and propanal in very small amount.[32]

2.3 Oxidation processes: HOR, MOR, FAOR.

2.3.1 Hydrogen oxidation reaction (HOR).

The hydrogen oxidation reaction transforming hydrogen into protons can occur in both acid (R9) and alkaline media (R10). This reaction is much simpler than those described above.

$H_2 \rightarrow 2H^+ + 2e^-$	E° = 0 V vs RHE	(R15)
$2OH^- \rightarrow 2H_2O + 2e^-$	E° = 0.83 V vs RHE	(R16)

Pt is the most active catalytic surface for this reaction, notably in acidic media while a poorer activity is obtained in alkaline media due to much slower kinetics.[41,42] Efforts are made to address this issue with Pt-free metal surfaces.

2.3.2 Methanol oxidation reaction (MOR) and Formic Acid oxidation reaction (FAOR).

MOR and FAOR could be considered as coupled reactions since formic acid might be one of the intermediates in the MOR besides CO or CO_2 which are final products. These reactions are generally catalyzed by Pt or Pd-based materials.

Oxidation of formic acid could follow a direct pathway of dehydrogenation ($HCOOH \rightarrow HCOOH^* \rightarrow CO_2 + 2H^+ + 2e^-$) or an indirect pathway of dehydration ($HCOOH \rightarrow CO^* + H_2O \rightarrow CO_2 + 2H^+ + 2e^-$). In a third route ("formate pathway"), the adsorbed precursor HCOOH* is dehydrogenated to stable bridge-bonded adsorbed formate ($HCOOH \rightarrow .HCOOH^* \rightarrow HCOO^* + H^+ + e^- \rightarrow CO_2 + H^+ + e^-$).[43] Under acidic conditions at potentials between 0.2 and 0.4 V vs RHE with Pt as catalysts, the direct oxidation of weakly adsorbed HCOOH*species to CO_2 was proposed as the dominant reaction pathway according to spectroelectrochemical studies. Theoretical considerations have shown that the reaction pathways are highly sensitive to the "Pt atomic structure": 1-2 isolated atoms are required for the direct pathway while an ensemble Pt sites is needed for the indirect one.[44] MOR has a mechanism of multistep elementary reactions, ending to CO_2 as final products. However this reaction is obviously much more demanding than FAOR in which CO_2 is already in the molecular structure. Overall, MOR involves the transfer of six electrons with many surfaces intermediates, including CO*, HCHO*, COH*.[45] They can contribute to poison the surface, decreasing the efficiency of the process. Similarly, these species can also block the cathode. Pt-based systems (i.e. Pt-Ru) have very good activity and stability in acidic solution, and many mechanistic studies have been performed using these systems.[46,47] MOR can be also carried out in alkaline media, allowing notably the use of cheaper and less scarce metals as catalysts (Ni, Ag for instance). Actually, the catalytic performance is better in alkaline media because of the faster kinetics and less corrosive environment.[47]

3. Surface functionalization of single-metal catalysts.

3.1. Deliberate chemical modification of flat metallic surfaces.

There is only a few examples of chemical modification of flat surfaces with organics compared to the more numerous examples with nanomaterials. Flat surfaces are better considered for basic investigations than for developing applications. Namely, single crystal plane materials have well-defined surface atomic arrangement, making them "ideal" catalysts for a deep understanding of the reaction mechanisms and surface processes.[48,49] It is then interesting to consider the impact of surface modification on such electrodes by screening different surface modifiers and electrocatalytic reactions. Some examples are gathered below and organized according to the approaches employed for surface modification. Various effects of the surface modification could be deduced from these examples and they do not necessarily correlate with the surface modification strategy.

Electrostatic and physical adsorptions. Adsorption of organic cations or neutral polymers onto Cu surfaces allows the tuning of the selectivity of CO_2 reduction (CO_2RR) in aqueous potassium carbonate (pH =6.8) according to their protic/aprotic and/or hydrophilic/hydrophobic natures, showing the importance of the hydrophilic/hydrophobic nature of interfaces compared to unfunctionalized oxide-derived Cu surface.[50] The hydrophilic/hydrophobic nature was classified on the basis of contact angle measurements by taking the unfunctionalized oxide-derived Cu as the reference. The aprotic species are demonstrated to limit the competitive HER process from 97 % down to 3%, in contrast to protic species.[50] Among the aprotic species, hydrophilic species improved selectivity to formic acid up to 62 % while cationic hydrophobic ones favor formation of CO with yield reaching 76 %.[50]

Electropolymerization. Electrochemical deposition of polymers, namely polyaniline, polycarbazole, polypyrrole and polyindole at platinum electrode is found to promote the direct oxidation of formic acid (FAOR) at low potentials in acidic medium, according to a pathway that does not involve CO as intermediates. The polymer layers inhibit the formation of poisonous CO*, allowing the direct pathway to occur.[51]

Chemisorption through chelate effect. Enhancement of selectivity is also reported thanks to a chelate effect of benzimidazole (BIM) at copper surface.[52] The conversion of CO_2 to C_2/C_3 products is observed together with a drastic decrease of the HER process with a much higher yield than bare copper at -1.07 V vs RHE. This enhanced selectivity is ascribed to the formation of a thick $Cu(BMI)_x$ layer which is supposed to i) restrict the proton diffusion, hence increases the local pH at the catalyst surface to suppress HER and ii) be a source of active $H^{\delta+}$ orienting the intermediates formation towards C_2/C_3 products.[52] Interestingly, the analysis of current density and ESCA indicates that underlying Cu surfaces rather than Cu(BIM)x complexes are the active surface.

Another chelate effect has been described on Pd surface with tris-N-heterocyclic carbenes (NHC) (Figure 1). This surface modification is found to boost the electrochemical reduction of CO_2 to C_1 products (82 % formate and 4 % CO) with high efficiency compared to bare palladium (32-fold increase and FE =86 % vs 23 % for unfunctionalized Pd) together with a better stability over 6h.[53]

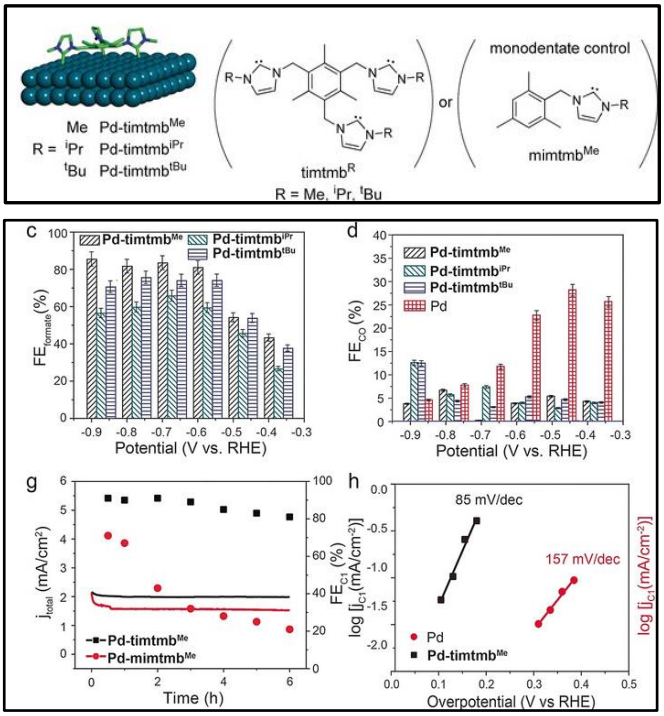

Figure 1. *(**top**) Schematic illustration of the functionalisation of Pd surfaces with NHC ligands. (**bottom**) (c) FEs of formate generation by the Pd modified electrodes (d) FEs of CO generation by the bare Pd and modified Pd electrodes (g) CPE of tridentate-NHC Pd-mimtmbMe and monodentate-NHC Pd-timtmbMe electrodes at −0.57 V over a 6 h time course (h) Tafel plots of Pd and Pd-timtmbMe electrodes. Adapted from ref [53] copyright Wiley VCH*

Despite a smaller electrochemical active surface (ESCA) *vs.* bare palladium, higher activity and selectivity are obtained on the chelated palladium, showing the high intrinsic activity of the molecular-materials interfaces formed by NHC ligation. Interestingly, CO stripping used for ESCA determination evidences an increase of electron density on Pd surface by NHC grafting, suggesting also an electronic effect contribution. [53] As additional examples of chelating systems, we could quote the adsorption of 5-diamino-1,2,4-triazole and citric acid (that is a well-known chelating agent used for depositing metals) on silver and nickel electrodes, respectively. The two modified electrodes display better catalytic performance towards CO_2RR [54] and OER, [55] respectively.

Self-assembly. Self-assembled monolayers of thiols groups (SAM) was also employed for the deliberate chemical functionalization of flat bulk gold, platinum and copper electrocatalysts.[56-60] Thus, gold electrodes involved in the electrochemical reduction of CO_2 in aqueous 0.1 M HCO_3 are modified with 2-mercaptopropionic acid (MPA), 4-pyridylethylmercaptan (4-PEM) and cysteamine (CYS).[60] The selectivity of the reaction is found to strongly depend on the nature of the ligands.[60] Gold electrode modified with SAM of 4-PEM shows a two-fold increase in FE and a three-fold increase in formate production compared to bare Au. In sharp contrast, the gold electrode with SAM of MPA displays an almost 100 % FE for HER while the electrode modified with CYS has an intermediary behavior, increasing both CO and H^+ production but without any change in the selectivity.[60] The pKa of the ligands is suggested to correlate with the yields of produced formate and H_2.[60] Ligands with low pKa (MPA) favor the HER through facile proton

donation. Ligands with high pKa (CYS) result in diminished protonation, and thus the product selectivity remains unchanged compared to bare electrode. The intermediate pKa of 4-PEM facilitates the proton transfer to CO_2 in a way that yields formate through a proton-induced mechanism (see Figure 2).

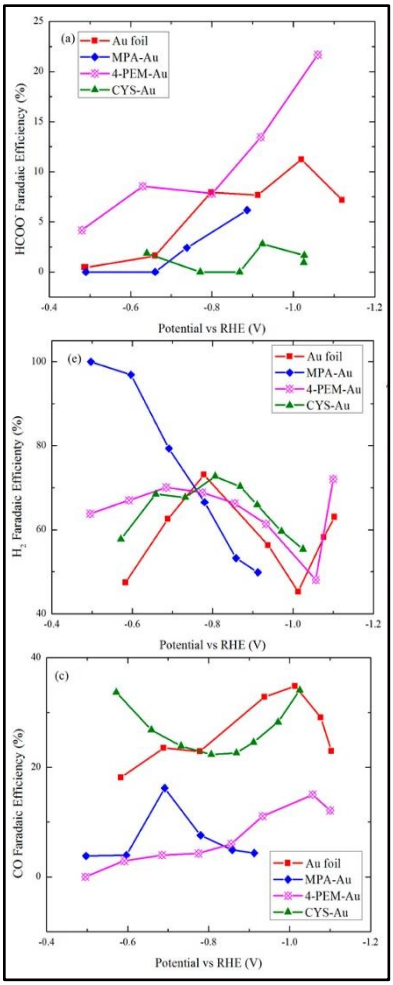

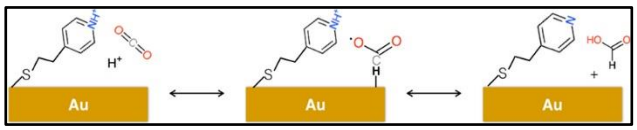

Figure 2. (top) Faradic efficiencies at bare polycristalline and thiolates modified gold electrodes (MPA =2-mercaptopropionic acid, 4-PEM = 4-pyridylethylmercaptan, CYS= Cysteamine) for (a) formate (b) H_2 (c) CO formation (bottom) Proposed formate formation mechanism during electrochemical reduction of CO_2 at a gold electrode modified with a SAM of 4-pyridylethylmercaptan. Adapted From ref [60] © 2017 American Chemical Society

Self-assembled (sub-)monolayers of thiolated calix[4]arenes were formed onto Pt(100), Pt(111) and polycrystalline Pt surfaces.[58] All the modified electrodes are found to be highly selective towards HOR process in acidic $HClO_4$ medium. The proper selection of surface coverage is crucial in this work since the selectivity arises from very strong ensemble effects.[58] High coverage of Pt(111) with SAM of calix[4]arene (98 % coverage) leads to an efficient blocking of ORR while the remaining Pt sites form a proper ensemble sites that is very active for the adsorption of H_2 and consequent H-H bond breaking.[58]

The self-assembly of another macrocycle, a tetrapodand metalloporphyrin, onto copper surface exemplifies a promising synergy of a metallic complex positioned at a remote but short distance of the catalyst surface, able to act with it.[59] This molecular design forms face-to-face cavities binding over a copper electrode but leaving catalytic sites available (Figure 3). This scaffold is thought to play a central role in enhancing the selectivity for electrochemical CO reduction to C_2 products and over competing water reaction. The selectivity is found to vary according to the length of bridging units and the nature of the metal in the porphyrin core. This suggests the involvement of hydrogen-bond interactions with the porphyrin cap and/or cooperative effect of the metal center in the mechanistic pathway. However, an electronic induced effect impacting the intermediates adsorption /desorption cannot be ruled out since the grafting of porphyrins onto the copper surface also induces an alteration of the local electronic structure as revealed by lead underpotential deposition and XPS experiments.

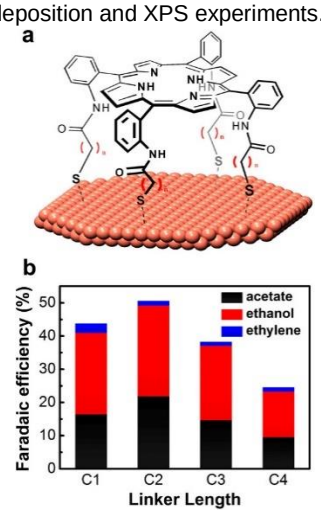

Figure 3. (a) Schematic illustration of free-base porphyrins possessing different linker lengths. (b) Faradaic efficiencies for CO reduction on Cu foils functionalized with free-base porphyrins possessing different linker lengths (Cu-H_2PCnSH). The electrolyses were performed at a constant potential of −0.55 V vs RHE in CO-saturated 0.1 M KOH (aq). From ref [59] © 2017 American Chemical Society

3.2. Molecular functionalization of nanomaterials.

Nanomaterials usually show enhanced activity compared to flat surfaces because of their morphological, electronic and chemical surface properties, namely high conductivity, large surface area and high stability under reductive potentials. Therefore, much more literature is available with the deliberate molecular functionalization of nanocatalysts. This section describes surface modification of single-metal nanomaterials and its effect on electrocatalysis main descriptors. After a short paragraph reporting the rare examples of surface modification evaluated both with flat bulk and nano- materials, we will successively consider CO_2RR, ORR and oxidation processes.

3.2.1 From flat materials to nanomaterials?

Importantly, the behavior of flat bulk materials can seldom be transferred to nanocatalysts because of the presence of much more different sites (steps, short-range terraces, etc) in nanomaterials. Thus, only two examples of organic ligands

employed with bulk flat surfaces [58,59] have been also evaluated with nanomaterials.[61,62]

The functionalization of commercial NSTF (nanowire free of carbon support) and TKK (carbon-supported 5 nm nanoparticles) Pt nanocatalysts with calixarene-thiol leads to very similar behavior than with functionalized bulk platinum.[58] This suggests that the selectivity due to calixarene coverage is not affected by the specific stepped structure of nanomaterials. In addition, the activity toward HOR is high and similar to calixarene-free Pt surface.[61] A main point is the very good electrochemical stability of the nanocatalytic system when exposed to an oxygen-rich environment at 0.8 V for 14 h at 60 °C, which are conditions somewhat harsher than those usually undergo in real fuel-cell system.[61]

Following the work on copper surfaces,[59] the tetrapodand thiol-terminated porphyrins were also used as chelating ligands for gold nanoparticles (7.2 nm). [62] But, in this work, only free-metal porphyrins ligands were used while the electrocatalytic reduction of CO_2 to CO was considered. The gold nanoparticles functionalized with the tetradentate porphyrin ligands show a 110-fold enhancement of the specific CO current density (~ 2.3-2.5 mA/cm^2) compared to their parent oleylamine–coated gold nanoparticles at -0.45 V vs RHE. The faradaic efficiency is 93 % while only 13% is obtained with oleylamine coated NPs. The porphyrin coated nanoparticles are even more efficient than naked gold nanoparticles prepared by the removal of surface oleylamine and used for control experiments (FE = 45 % and J_{CO} = 0.5 mA/cm^2).[62] The authors also show a very good stability without deactivation during 72 hours of electrolysis.[62] A further interesting point is that the reduction mechanism is basically impacted by the nature of the ligands as revealed by Tafel analysis .A Tafel slope of 123 mV/decade is observed in the case of oleylamine-capped nanoparticles in agreement with an initial rate-determining electron transfer to adsorbed CO_2 to form adsorbed anion radical $CO_2^{\bullet-}$ (theoretical 118 mV/decade).[63,64] In contrast, the Tafel slope for porphyrins modified nanoparticles is only 69 mV/decade, suggesting that the nanoparticles might undergo a pre-equilibrating one-electron transfer followed by a rate-limiting chemical step (theoretical 59 mV/decade).[63,64]

3.2.2 Modification of nanocatalysts involved in CO_2RR.

A similar behavior has been evidenced in another study of Chang and co-workers, considering gold nanoparticles functionalized with N-heterocyclic carbene (NHC) which were subsequently involved in electrochemical reduction of CO_2).[65] The NHC-capped nanoparticles displayed an improved FE (83 %) for reduction of CO_2 to CO at -0.57 V vs RHE with a 7.6 fold-increase of current density compared to that of parent oleylamine gold nanoparticles (FE =53 %). It is accompanied with a decrease of the Tafel slope from 138 mV/decade (oleylamine-capped NPs) to 72 mV/decade (NHC-capped NPs), showing once again that the molecular ligand influences mechanistic pathway.[65] The authors proposed that strong σ-donation from the carbene made the gold nanoparticles highly electron-rich, explaining the observed change in mechanism. The strong carbene-gold bond can destabilize gold-gold bonding with neighboring atoms, leading to surface restructuration by increasing the numbers of defects which are reactive sites for the CO_2 reduction (Figure 4). This has a direct impact on the adsorption/desorption processes of intermediates species. A better kinetics for the electron transfer to CO_2 could be then reached, allowing fast electron transfer to CO_2 to occur prior to the rate-determining step.

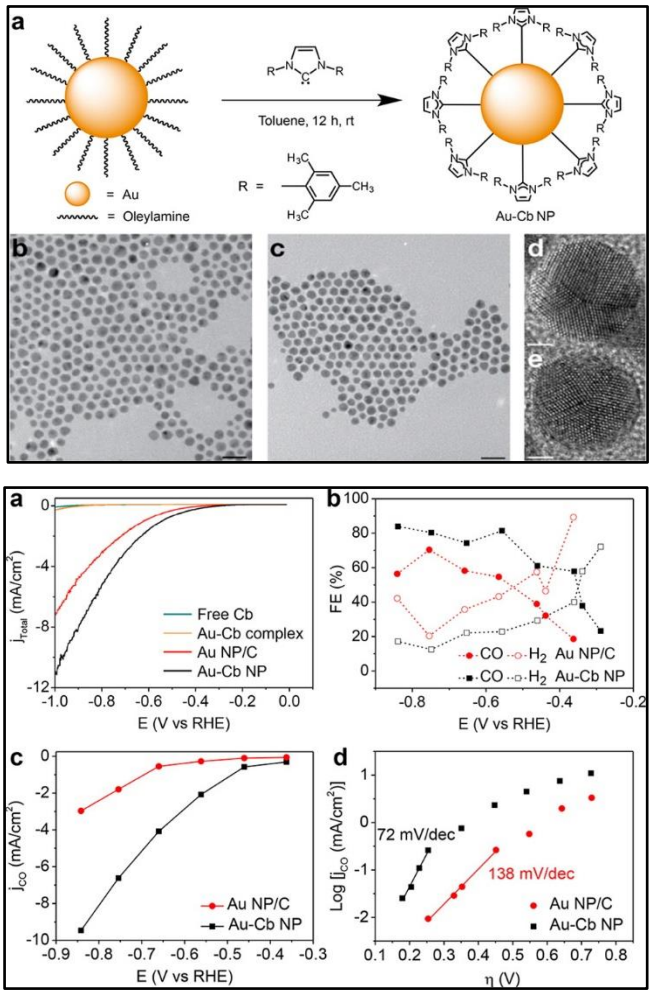

Figure 4. (**top**) Scheme of ligand exchange reaction on Au NPs capped with oleylamine to form NHC-capped Au NPs. Below are the characteristic TEM and HRTEM images of NPs (oleylamine NPs (b and d); NHC NPs (c and e)). (**bottom**) (a) LSV scans of Au–NHC NP (*Au-Cb*), Au NP/C, free carbene (*Cb*) and molecular Au–NHC complex (*Au-Cb complex*) under CO_2-saturated 0.1 M $KHCO_3$ at pH 6.8. (b) Faradaic efficiencies of products formed from Au–Cb NP and Au NP/C. (c) Specific CO current density (based on electrochemically active surface area) plots for Au–Cb NP and Au NP/C. (d) Tafel plots of Au–Cb NP and Au NP/C. From ref [65] © 2016 American Chemical Society

Carbon-supported gold nanoparticles modified through the adsorption of polymeric polyvinyl alcohol (PVA) show better activity and selectivity than the corresponding naked nanoparticles.[66] Herein again, Tafel analysis indicates that the PVA modification on the nanoparticles (with moderate coverage) induces a most favorable reaction pathway for CO_2RR. The great performance of this catalytic system is ascribed to the formation of an hydrogen-bond network from the metal polymer interface which both increases the activity of CO_2RR by stabilizing key intermediates and inhibits HER.[66] The PVA coverage density is found to play a key role with an optimal coverage of 20 % for having the best mass and current specific activities. This illustrates the necessity of regulating the surfactant coverage density.[66]

Chemical modification has been also applied to ultrasmall gold nanoparticles (~ 2 nm), by employing linear and branched amine ligands [67] or hydroxyl-terminated poly(amidoamine) dendrimers.[68] Both works demonstrate a better selectivity for the CO_2 to CO conversion with linear amines and lower generation dendrimers. In contrast, branched polyamine (polyethyleneimine) or higher generation dendrimers hindered CO formation and improved HER.[67,68] One reason may be a larger surface coverage with these latter compounds.[67] But a second point could be invoked. Indeed, authors have reported a substantial size growth of the nanoparticles modified with the linear amine and low dendrimers during the electrolysis. In contrast, high-generation dendrimers stabilized the nanoparticles that almost kept their initial size.[68] This work illustrates the gain of stability thanks to the molecular functionalization, allowing the preservation of the nanoparticles size. Finally, it comes that ultrasmall gold nanoparticles favor HER compared to larger nanoparticles.[69]

Cysteamine is employed as anchoring agent for the one-pot synthesis of silver nanoparticles on carbon support.[70] The resulting catalytic system shows improved activity and durability for CO_2 conversion to CO, notably a decrease of the overpotential that is a major issue with Ag catalysts. On the basis of DFT calculations, the authors propose that the cysteamine modifies the spatial spin density of the Ag nanoparticles owing to Ag-S interaction. This induces favorable intermediates stabilization, which decreases the overpotential.[70] More interestingly, the same authors have evaluated the effect of the binding interactions of capping ligands having different anchoring groups, i.e. amine, carboxylic or thiol functional groups (Figure 5).[71] Amine- (oleylamine) and carboxylic- (oleic acid) functionalized silver nanoparticles showed superior CO activity than the dodecanethiol-capped particles, with the best performance obtained for the amine modified nanoparticles. These latter delivered a high FE (94 %) for CO production along with a suppression of HER whereas the thiols capped systems increased both the HER and CO_2RR activities. DFT calculations suggested that the amine-capped ligands stabilized the *COOH intermediate, destabilized H binding and then suppressed HER while thiol ligands indiscriminately increased HER and CO_2RR, hence *de facto* lowered the FE for CO production.[71]

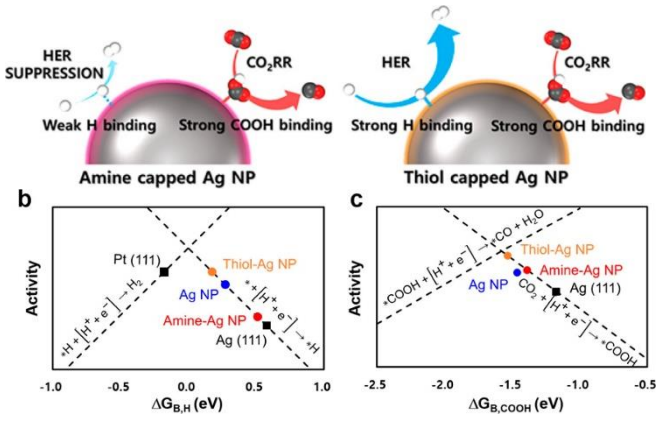

Figure 5. (**top**) Schematic representation of amine- and thiol- capped silver nanoparticles and their related CO_2RR and HER activities. (**bottom**). (b) Volcano plot of HER, shown as a function of the hydrogen binding free energy (ΔGB,H), for Ag nanoparticle (Ag NP), thiol-capped Ag NP, and amine-capped Ag NP, respectively. (c) Volcano plot of CO_2 reduction reaction, shown as a function of COOH binding free energy (ΔGB,COOH) for Ag NP, thiol-capped Ag NP, and amine-capped Ag NP, respectively. Dashed lines show the activities of each elementary step. From ref [71] © 2016 American Chemical Society

A very interesting design of molecular ligand for decorating silver nanocrystals has been proposed recently.[72] The organic ligand consists of a disubstituted imidazolium bearing an anchoring group on one side and an alkyl chain on the other side. This specific design allows (i) the variation of anchoring group in order to study the possible impact of the functional binding group in the local electronic structure of the surface, (ii) the use of imidazolium as a carbon-capture motif to encourage the reduction of CO_2 to CO and (iii) the variation of the alkyl tail length in order to modulate the interactions at the solid/liquid interface. This work brings interesting fundamental insights on the molecular tuning of surface catalysts. Results show that both the manipulation of local electronic structure due to anchoring groups, along with the solid/liquid interface with alkyl tails are of importance in obtaining high selectivities.[72] High FEs for CO at 1.1 V (92 %) with a specific activity of 256 μA cm^{-1} are reported, making these systems highly competitive regarding silver catalysts in the literature while having better performances compared to corresponding non-functionalized silver nanocrystals.[72]

Considering now Cu surfaces, a work by Wang and collaborators discriminates materials morphology *vs* ligands effects.[73] A polished Cu foil, a Cu nanowire and an annealed Cu electrode were modified with amino acids for the selective electroreduction of CO_2 to hydrocarbons. For all the three electrodes, amino acids modification allows a remarkable enhancement of the efficiency of the formation of total hydrocarbons and an inhibition of HER, regardless of the morphology of the Cu electrodes. By considering glycine as a model (simplest amino acid), theoretical calculations indicate that adsorbed CHO intermediates can be stabilized through the formation of hydrogen bond with the $-NH_3^+$ moiety of glycine, hence enhancing the selectivity.[73] The stabilization of adsorbed intermediates CHO* or *COH over that of adsorbed *CO is crucial to competitively form hydrocarbons.[74]
Polydopamine coated Cu nanowires were also shown to promote an enhanced selectivity towards the production of CH_4 compared to unfunctionalized Cu nanowires while polydopamine itself have poor catalytic activity.[75] FEs for CH_4 increase with the polymer film thickness providing that the film still permits the permeation of CO_2, i.e. for thickness below 40 nm. Strong interaction between polydopamine and Cu nanowires is evidenced to be of significance in the product selectivity. Finally, these catalysts show an exceptional stability over 14 h electrolysis, in addition to strong resistance against oxidation after three-month storage in air.[75]

3.2.3 Modification of nanocatalysts for ORR.

The surface modification of nanocatalysts has been even more largely used and studied for ORR process, mainly for Pt,[76] or Au materials as reviewed in the two following subsections.

3.2.3.1 Platinum.

The ORR over Pt nanoparticles in acidic media is an archetypal structure-sensitive reaction, with optimal particle sizes in the range 2-4 nm.[77-80] The presence of organic ligands at the Pt surfaces is likely to impact the adsorption and dissociation energetics of O_2 and oxygenated intermediates (O*, OH*, OOH*, HOO*) that govern the activity and selectivity of the electrocatalytic processes, whatever the underlying associated mechanisms.[22] A wide range of organic compounds such as surfactants,[81,82] polymers,[83-85], capping ligands[86-99] or adsorbed macrocycle[100] were demonstrated to tune the reactivity of Pt nanoparticles.

Overall, the effect of the chemisorption or grafting of organics onto the Pt nanocatalysts were mainly attributed to local modification of the electronic properties of the surface. Some striking examples are described below. First, the reductive grafting of aryldiazonium salts were employed to modify Pt nanoparticles by Chen and co-workers.[86,87] Using 4-chlorophenyl diazonium salt, they synthesized chlorophenyl stabilized Pt nanoparticles supported on carbon (Pt-ArCl) and modified commercial Pt/C (Pt/C^{ArCl}).[87] In both cases, the electron-withdrawing chlorophenyl groups form a multilayer structure on the nanoparticle surface. The functionalized nanoparticles exhibit improved ORR electrocatalytic activity compared to naked commercial Pt/C nanoparticles. Despite a smaller size (1.85 nm vs 3 nm for commercial Pt/C), Pt-ArCl nanoparticles have a 2.3 times higher specific activity and a 2.8 times higher mass activity at 0.9 V vs RHE. This point is remarkable because ORR activity is known to typically decrease with decreasing particle size in case of naked Pt nanoparticles.[101,102] Similarly, Pt/C^{ArCl} doubled the mass activity and tripled the specific activity for ORR. To better understand the fundamental mechanism, Chen and co-workers have further studied the ORR activity of aryl-stabilized Pt nanoparticles of same core size with different *para*-substituents (R) of increasing electronegativity (CH_3, F, Cl, OCF_3, CF_3).[86] By correlating the Hammett substituent constant (σ) with the ORR mass and specific activities at 0.9 V vs RHE, it is shown that the electron-withdrawing capability of the ligands plays a key role in controlling the ORR activity. The larger σ, the higher are the mass and specific activities (**Table 1**).[86]

Table 1. Physical parameters of Aryl stabilized Pt nanoparticles and their corresponding specific (jk) and mass (jm) activities for ORR at 0.9 V. From ref [86]

R	CH_3	F	Cl	OCF_3	CF_3	Ø[a]
σ	-0.017	+0.05	+0.23	+0.35	+0.54	
Part. Size (nm)	2.1	2.1	1.85	2.5	2.2	3.3
ECSA ($m^2\ g^{-1}_{Pt}$)	54	54	93	47	59	80
J_k ($mA\ cm^{-2}$)	0.15	0.30	0.47	0.52	0.65	0.20
Jm ($mA\ mg^{-1}_{Pt}$)	0.082	0.162	0.437	0.244	0.384	0.16

[a] commercial Pt/C

The activities of the most “electronegative” samples are much larger than that of commercial Pt/C. The aryl functionalization with electron-withdrawing group is suggested to change the electronic structure of the Pt nanoparticles by decreasing the electron density of the Pt surface atoms. Indeed, for oxygen adsorption on Pt, electron is transferred from Pt to oxygen. The electron-withdrawing ligands weakened the adsorption of oxygenated intermediates (O* or OH*) on the Pt surface which are central in the mechanistic pathway.[103] This should favor ORR catalytic ability since the reductive desorption of adsorbed oxygen species to form water is thought to be the sluggish step during the process on platinum surface.[104]

Close results have been earlier described with triphenyl phosphine triphosphonate (TPPTP) capped platinum nanoparticles.[89-92] Organophosphine ligands have rich transition-metal coordination chemistry, being σ donors and π acceptors, capable of forming $p\pi$-$d\pi$ phosphorous-metal bonds, notably with platinum. In acidic medium, the smaller TPPTP nanoparticles perform better than bare Pt catalyst (2.4 nm) and similar to large commercial one (4.4 nm), with a clear enhancement of the ORR kinetics. [89,90,92] The authors proved from X-ray absorption spectroscopy measurements that a majority of Pt sites was involved in strong electronic coupling with TPPTP through Pt-O-P<tp linkage.[91] This causes a weakening of Pt-O* at the modified nanoparticles surface. Apart electronic effects, the authors argued that the hydrophobic nature of TPPTP ligands reduced the water concentration near the surface and limited the Pt-oxide formation. All these reasons contribute to enhanced ORR activity despite a strong blocking of Pt sites.[91]

In another work, Chen and co-workers synthesized platinum nanoparticles capped with acetylene derivatives (1-alkynes, 4-ethylphenylacetylene (EPA), 4-tert-butylphenylacetylene(BPA)).[88] The capped nanoparticles show improved performance for ORR activity, in alkaline media, in terms of onset potential and kinetic current density compared to the naked commercial Pt/C catalysts.[88] For instance, the normalized kinetic current densities at -0.18 V vs Hg/HgO were 12.6 $mA.cm^{-2}$ (Pt-BPA), 19.1 $mA.cm^{-2}$ (Pt-EPA), 12.3 $mA.cm^{-2}$ (Pt-1-decyne) and 4.1 $mA.cm^{-2}$ for commercial Pt/C. Strong coupling

between the ligands and the metallic surface arises from the formation of conjugated $Pt_{surface}$-C≡ at the metal-ligand interface, resulting in extensive spilling of the Pt core electrons to the ligands shells. This is more effective for 4-ethylphenylacetylene and 4-*tert*-butylphenylacetylene than for 1-alkynes. Actually, the temperature dependence of the ensemble conductivity is in agreement with a semiconducting character in the case of nanoparticles stabilized with 1-alkynes and 4-ethylphenylacetylene whereas a metallic behavior is observed for the 4-*tert*-butylphenylacetylene, probably because the sterically hindered and electron donating *tert*-butyl groups facilitates the intraparticle charge transfer. The surface functionalization is then demonstrated to induce a manipulation of the Pt core electronic structure that impacts the bonding interaction with adsorbed oxygen. Interestingly, the 4-ethylphenylacetylene-Pt nanoparticles exhibits the best electrocatalytic activity among the series as the best compromise between extensive intraparticle charge delocalization and accessibility of the Pt surface by electrolyte counterions.[88]

It is further interesting to consider another work of Chen's group that balances impact of surface modification with the structure of the nanoparticles.[96] The chemisorption of *para*-substituted styrene derivatives onto Pt nanoparticles surfaces allows the formation of strongly stabilized Pt nanoparticles through platinum-vinylidene/ or platinum–acetylide interfacial bonds, hence with strong electronic coupling (Figure 6).[96] The electrocatalytic activity towards ORR in acidic media decreases sharply with *para* substituents in the order methoxy << trifluoromethyl < -*tert*-butyl.[96] Although that *tert*-butyl group has a lower Hammett constant (σ = -0.20) than the trifluoromethyl group (σ = +0.54), these nanoparticles have the best performance. Such a result is in apparent contradiction of earlier work of the same group.[86] However, the *para* substituents are found to impact the size of the resulting nanoparticles and the trifluoromethyl substituent also lead to the smaller nanoparticle. Therefore, these results suggest that the core size has a potent effect in the ORR activity, beyond any electronic structure manipulation.[86]

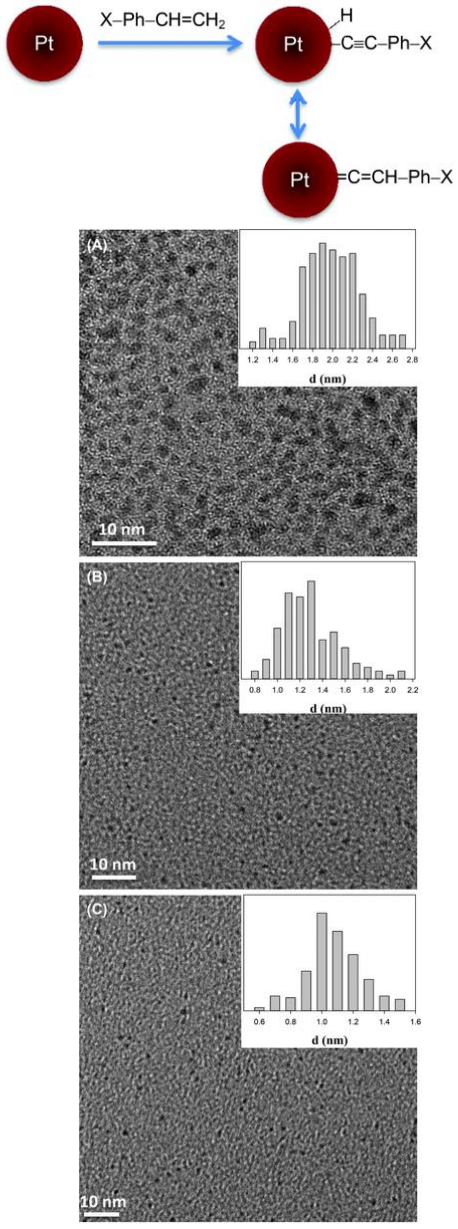

Figure 6. Functionalization of Pt nanoparticles through dehydrogenation of styrene derivatives to acetylene moieties capable of self-assembly onto Pt nanoparticles and representative TEM images of Pt NPs with substituents (A) tert-butyl, (B) methoxy and (C) trifluoromethyl. Scale bars are all 10 nm. Insets are the corresponding core size histograms. From ref [96] copyright The Royal Society of Chemistry 2016

Small amount of oleylamine chemisorbed onto platinum nanoparticles allows a significant enhancement of the ORR activity in acidic solution.[93] Despite a significant loss of ESCA, the kinetic current density is over 3 times higher than that of unmodified particles.[93] These effects are rationalized with changes in the electronic structure of the frontier d-band (Figure 7). By combining synchrotron-based photoelectron spectroscopy (PES) and X-ray absorption fine structure spectroscopy (XAFS), an alteration of the d-band structure was observed that took place by increasing electron density in the frontier d states of Pt and caused downshift of the d band. The modification of the frontier d-band structure is due to an electronic effect involving the donation

of electrons from organic species (oleylamine) toward Pt nanoparticles. Interestingly, the downshift of the d band center is proportional to the increase of surface coverage, suggesting that an optimal interaction between reactants and catalysts is dependent of surface coverages. A negative shift of the d-band center indicates that intermediates species weakly interact with the Pt surface, rendering the kinetics of ORR more facile.

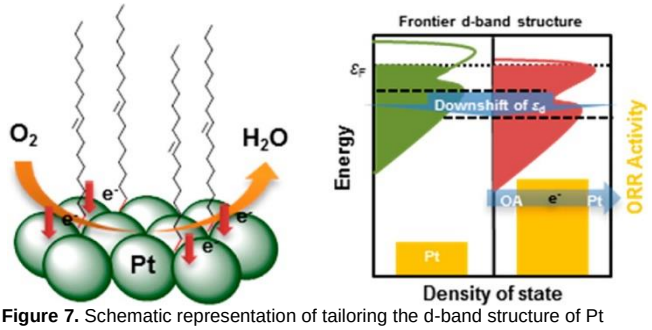

Figure 7. Schematic representation of tailoring the d-band structure of Pt nanoparticles by oleylamine capping agents.from ref [93] copyright ACS 2013

While local modification of the electronic properties is a widely considered effect of surface modification, other effects explaining the better ORR activity have been also put forward. For instance, the presence of oleylamine capping molecules prevents the adsorption of phosphate anions that can severely deactivate ORR process. In a further work, the same authors highlighted a third-body effect to explain the tolerance of oleylamine-modified Pt nanoparticles toward phosphate anions.[82] Oleylamine possesses bulky aliphatic chains able to selectively block the adsorption of large anions such as phosphate while granting access to small oxygen molecules. Such a result is particularly interesting for application in high-temperature PEMFCs that utilize polybenzimidazole membranes doped with phosphoric acid.

Indeed, preventing the adsorption of poisonous species on electrocatalysts also contribute to increase the performance of fuel cells, which mainly employ Pt as cathode catalysts. Thus, Yoo and co-workers have modified Pt nanoparticles with zwitterionic L-cysteine molecules.[94] L-cysteine is chemisorbed on Pt surface through a thiolate-Pt bond. Using an optimized surface coverage, they found better half-wave potentials, mass and specific activities for the modified Pt nanocatalysts than for the naked ones both in aqueous 0.05 M H_3PO_4 and 0.1 M KOH electrolytes. Direct electrostatic interactions with spectator poisonous ions could be modulated through the protonation/deprotonation of amine and carboxylic acid *termini* of the cysteine in KOH and H_3PO_4 solutions, respectively. Inhibitor ions (excess of OH and bulky hydrated K^+ or phosphoric acid oxyanion) are thus successfully ruled out,[94] with possible applications in alkaline (AFC) and in phosphoric acid (PAFC) fuel cells.

In the following two examples, the contribution of the chemical functionalization of Pt nanoparticles is also supposed to affect the local solubility of O_2 at the surface. Mixed layers of octylamine (OA) and 8-(pyren-1yl-methoxy)octane-1-amine (PA) chemisorbed onto platinum nanoparticles are demonstrated to increase the stability and the electrocatalytic ORR activity (both specific and mass activities) compared to bare Pt.[97,99] The authors explained the high ORR activity of their OA/PA modified nanocatalysts by a change of the adsorption kinetics of intermediates and/or of concentration of oxygen adjacent to the Pt nanoparticles surface. They then use perfluorinated alkylamines.[98] The resulting modified platinum nanoparticles show high ORR activity and durability in acidic solution compared to commercial catalyst. Besides suppression or weakening of undesired oxide formation at the Pt surface, the presence of perfluorinated chains are supposed to increase the O_2 solubility next to the surface and to enhance the affinity with Nafion, allowing the creation of proton conduction path.[98] Such solubility effect associated to the chemical modification may be sensitive to packing and surface coverage. Polyethyleneglycol (PEG) chains with pendant amino acid groups were immobilized onto platinum nanoparticles. A significant improvement of the ORR activities is observed compared to bare metal, even at high PEG loadings.[95] However, the ORR performance depends on the nature of the amino acids and its end functional group.[95] Especially, the presence of amide bonds in the ligand backbone avoids a tight packing of the PEG chains on the Pt surface, sustaining facile O_2 diffusivity.[95]

The effect of surface coverage was examined by controllably tuning the surface coverage of pyridine on Pt nanoparticles.[105] With an optimal surface coverage, the authors were able to prepare an effective bifunctional catalyst for direct methanol fuel cells. The catalyst exhibits both improved ORR activity and methanol oxidation tolerance. In light of DFT calculations, the variation of activity with pyridine surface coverage is due to a competition or cooperation between electronic and steric effects. Four other ligands (i.e. oleylamine, butylamine, 4-dimethylaminopyridine and triphenylphosphine) have the same behaviors.[105]

In another example using a polymer coating, the surface modification was also directed to protect the carbon support which may be deleterious for the catalyst performance. Polyaniline (PANI) was *in situ* polymerized onto Pt/C catalyst to form a polyaniline-decorated Pt/C@PANI core-shell structure.[85] The PANI layer selectively covers the surface of the carbon support more than that of Pt. For optimized PANI shell (thickness of 5 nm), both ORR activity and durability in acidic media are improved compared to unmodified Pt/C.[85] The authors attributed these significant improvements to the PANI-coated core shell structure, which induces electron delocalization between the Pt d orbitals and the PANI π-conjugated ligand, promoting electron transfer from Pt to PANI but also protecting the carbon support from direct exposure to corrosive environment.

Pt nanostructures of higher dimensionality. Chen and co-workers reported the synthesis of polyallylamine (PAA) functionalized Pt nanocubes,[84] Pt nanolances,[106] and long-spined sea-urchin like (LSSU) nanostructures.[83] While PAA-nanocubes and -nanolances have much lower ESCA than Pt black, [84,106] the Pt-LSSUs showed comparable values,[83] despite much bigger particle size (180 nm vs 8.6 nm for Pt black). This is due to high branching structure and sheet morphology of the branch.[83] In all cases, the authors evidence a strong coupling between platinum material and PAA. Notably, XPS measurements display a negative shift of the Pt binding energy of the modified Pt materials compared to bare platinum, which reflect a downshift of the d band center. The core level spectrum of N1s photoelectron reveals interaction between Pt and amine group of PAA. Lone pair electrons of the $–NH_2$ groups facilitate the transfer

of electrons from N to Pt atoms, decreasing the 5d vacancies in Pt. As a result of this strong interaction, the catalysts show greater specific activity and more positive shift of half-wave potentials compared to commercial Pt black.[83,84,106] The presence of PAA probably induces a weaker hydroxyl adsorption and an increase of interface proton concentration. Pt nanolances and Pt-LSSUs exhibit excellent durability thanks to their interconnected structures of nanoensembles prone to effective antioxidation features and strong interaction between the metal and amine group of PAA.[83,106] They are also highly tolerant to alcohol oxidation, showing their superior selectivity for ORR. Indeed, platinum is not selective to ORR, being also able to catalyze alcohol oxidation and this is the cause of alcohol oxidation crossover issues in direct alcohol fuel cells (DAFCs).

3.2.3.2 Gold.

In contrast to platinum, bulk gold is generally considered as a poor catalyst for ORR because gold has a filled d-band inducing weak adsorption properties.[8,22] However, gold nanoparticles exhibit remarkable catalytic activities for ORR, especially in alkaline media.[107] Kinetics and mechanisms of ORR on Au electrodes are strongly influenced by pH and crystallographic orientation.[107] Size of the particles is reported to be a major parameter for increasing performances. Surface-capping ligands are also an important point, especially because colloidal synthesis methods are widely used for preparing gold nanoparticles of different size.

Very recently, the catalytic activity of citrate-stabilized nanoparticles was examined as a function of their size, ranging from 15 nm to 95 nm.[108] A clear core-size dependency is observed for both onset potentials and kinetic currents. As expected, the smallest (15 nm) nanoparticles give the best electrocatalytic efficiency.[108] In addition, their electrocatalytic efficiency is comparable to those obtained for small Au clusters incorporating organic ligands ($Au_{55}Cl_6(PPh_3)_{12}$).[109] If these examples illustrate the strong impact of the core size in the case of gold nanoparticles, Xu and Zhang found that the nature of capping agents significantly outweighed the effect of particle size.[110] On the basis of similar particle sizes and internal crystal structures, they show that particles stabilized by polyvinylalcohol (PVA) and citrate have much higher ORR activities in aqueous KOH than those prepared with polyvinylpyrrolidone (PVP).[110] XPS measurements reveal that the Au 4f binding energy in nanoparticles capped with PVP is lowered by 0.9 eV compared to bulk Au while nanoparticles stabilized by citrate or PVA show no difference. Due to this effect, the PVP-capped gold nanoparticles may bind oxygen species too tightly, explaining the lower catalytic activity.[110] In the same context, the effect of the nature of “classical” capping agents (citrate, cetyltrimethylammonium bromide (CTAB), polystyrenesulfonate (PSS) and 11-mercaptoundecanoic acid (MUA)) has been investigated with nanoparticles having the same core size (15 nm).[111] The presence of the ligands is found to negatively shift the Au 4f binding energies compared to bulk gold, including gold nanoparticles capped with citrate. The largest shifts are observed for CTAB and MUA.[111] Such an observation suggests a local modification of the electronic properties of the gold surface due to chemical functionalization. The best catalytic performance for ORR is manifested by citrate capped nanoparticles whereas the lowest one is exhibited by PSS capped nanoparticles.[111] XPS analysis of the stabilized gold nanoparticles is performed after ORR measurements. The oxidation state of the gold core does not vary but gold capped with citrate or PSS show significant loss of the surface coverage of ligands, in sharp contrast with nanoparticles stabilized with CTAB and MUA. Lead underpotential deposition shows that citrate capped nanoparticles present (100) symmetry while the three other systems display mainly (111) domains. After ORR measurements, significant faceting transformation is observed with the citrate capped nanoparticles that acquire (111) symmetry while the other ligand-stabilized nanoparticles show almost no difference.[111] It is now established that the most active facets for 4-electron ORR pathway is the (100) domains.[8,112-114] Should faceting possibly assisted by adsorption/desorption of ligands be the driving force? Actually, oleylamine capped gold nanoparticles of 3, 6, 8 nm size mainly presented (111) facets, especially the 8 nm nanoparticles with twenty (111) facets and many defects.[115] But all show ORR activity, without any ligands removal treatment.[115] Surprisingly, the largest nanoparticles (8 nm), hence having the more (111) facets, are the most active. The authors attributed this increased activity to higher degree of disorder on the surface of the polycrystalline structure and to the ease of oleylamine removal during ORR process although that no experimental evidence was actually given to prove the loss of ligands.[115]

Others examples of ligand effect with more sophisticated architecture could be found. Gold nanoparticles were dispersed onto single-walled carbon nanotubes by supramolecular assembly involving an amphiphilic peptide. The gold nanoparticles were bound to the carbon nanotubes from thiol group of cysteine residue.[116] The resulting nanohybrids display improved ORR performance compared to bulk gold and even to commercial Pt/C catalysts. In addition to a better stability, size control and good dispersion, the peptide induces synergistic electronic effects as demonstrated by XPS and Raman spectroscopies.[116] The peptide behaves as a charge acceptor, resulting in partially positively charged gold. This can lead to the adsorption of O_2 by weakening the O-O bonding and thus facilitating the 4-electron pathway. A very similar behavior could be inferred from a work of Morozan *et al*.[117] (Figure 8). Gold nanoparticles were anchored and dispersed onto multi-walled carbon nanotubes thanks to the self-assembly of amphiphilic nitrilotriacetic-dyine lipid. In alkaline medium, the as-prepared nanohybrids are found to exhibit excellent ORR activity with a dominant 4-electron pathway, low overpotential and good stability.[117] While the impact of surface modification could be experimentally established, the effects sustaining this impact are not clearly addressed in all these above examples, except a possible electronic effect.

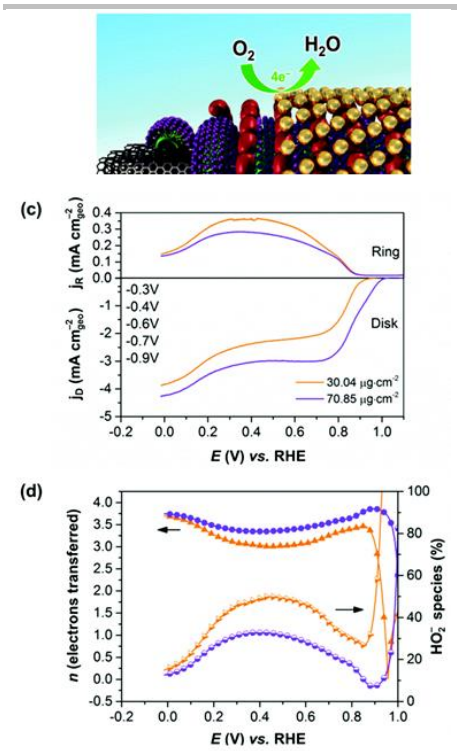

Figure 8. Nanohybrids with gold nanoparticles anchored to multi-walled carbon nanotubes through self-assembly of nitrilotriacetic-diyne lipid. (c) RRDE curves in a O_2-saturated 0.1 M KOH solution (10 mV s^{-1}, 1500 rpm, E_{ring} = 1.435 V *vs.* RHE) for two AuNP loadings ; (d) potential dependence of *n* (left scale) and of the ratio of HO_2^- produced (right scale). From ref [117] copyright The royal Society of Chemistry 2015

However, effects of ligands related to the modulation of the properties of the interface between electrolyte/reactants and metallic surface have been mentioned. Gold nanoparticles prepared by using cucurbituryl show promising activity towards ORR.[118] The organic cavities are prone to encapsulate dissolved dioxygen, allowing an increase of local concentration by nanoconfinement.[118] Robust gold nanoparticles modified from 4-decylbenzenediazonium salts are selective to the 2-electron pathway in ORR, producing H_2O_2 in alkaline medium, [119] because the grafted decylbenzene provides a local hydrophobic environment that stabilizes superoxide and peroxide formed.[119]

A recent paper from Fan and co-workers also highlighted the importance of surface coverage.[120] In some cases, surface coverage could even play a more significant role on ORR than particle size of gold nanoparticles.[120] In the same context, the nature and the number of organic ligands could be of fundamental importance for gold nanoclusters that displayed great potential in ORR electrocatalysis.[109,121] For instance, Sumner et al. have reported that even similar sized nanoclusters can display significant differences in catalytic activity, suggesting that other contributing factors, like ligands present in the nanoclusters precursors, can dictate the activity outcomes.[121]

3.2.3.3 Silver and Copper.

A few examples of modified silver[122,123] and copper[124] nanoparticles was also reported in ORR process. Metallophtalocyanines are described to modify the interface of silver nanoparticles supported on carbon. Compared to Ag/C, the modified silver catalysts have lower overpotentials and much lower Tafel slopes in the high overpotential region.[124] Similarly, organic ligands employed for anchoring silver nanoparticles on graphene are found to facilitate ORR in alkaline medium.[123] Stable alkyne-capped copper nanoparticles exhibit apparent electrocatalytic activity for ORR in alkaline medium, with higher activity than naked polycrystalline or single-crystalline Cu(100) and Cu(111) electrodes.[123]

3.2.4 Modification of nanocatalysts in oxidation processes (HOR, MOR, FAOR).

Similarly to Markovic and co-workers with calix[4]arene-thiols,[61] Yun *et al.* used dodecanethiol SAMs at a Pt/C catalyst.[125] The same selectivity towards HOR is found. The authors emphasized the difficulty to precisely "form the proper ensemble sites with just a particle-size control on sub-nanometer scale". Here again, the control of the surface coverage is thought to play a key role.

A very clever approach for promoting HOR was also recently proposed by Zhou and coll. and is based on the design of canopy-shaped molecular architecture.[126] 2,6-diacetylpyridine is strongly adsorbed on Pt surface through tridentate coordination, with the pyridine ring being in a titled orientation. This molecular structure provides a kind of canopy-shelter underneath the ring for Pt atoms, leaving accessibility of the small-sized H_2 while adsorption of relatively large CO and H_2S is inhibited.[126] CO and H_2S are very often present as impurities in H_2 production and are able to strongly deactivate the Pt catalyst. The canopied Pt nanocatalysts show enhanced performance for HOR, with an even greater CO tolerance than the most frequently used PtRu alloy catalysts.

Good CO tolerance is also a major challenge in MOR and FAOR, two important reactions for portable liquid fuel cells (Direct Methanol fuel cells and Direct Formic Acid fuel cells) for which Pt-based nanomaterials are the best electrocatalysts. The presence of organic ligands on Pt nanoparticles surface is shown to suppress efficiently the poisonous adsorption of CO, namely by using PVP,[127] polyethyleneimine,[128] adsorption of cucurbit[6]uril,[129] phenylacetylene derivatives,[130] pentyl-/tripentyl- amine,[131] or aryldiazonium salts.[132,133] In all these examples, the methanol and/or formic acid electrooxidation are greatly enhanced, outperforming processes with classical unmodified Pt nanocatalysts. However, these results are not systematically ascribed to a steric regulation of the active sites because the nature of the ligand itself and the surface coverage are also of importance and contribute to the better performance of the catalysts. Thus, Tong and co-workers suggest that the adsorption of PVP on the surface of Pt nanoparticles allows an enhanced water activation due to its hydrophilicity together with subtle electronic alterations.[127] They also propose that PVP induces additional reaction pathways for both MOR and FAOR. In contrast, Chen and co-workers who modified Pt but also Pd nanoparticles through reductive grafting of butylphenyldiazonium cations advocated for a suppression of CO poisoning rather than electronic effects to explain the better performance.[132,133] The authors observed comparable enhancement for Pt and Pd catalysts, more likely because butylphenyl moieties blocked the CO adsorption, probably through third-body effects.[132,133]

In addition, most of these works reported a rapid decay of the catalytic activities, but once reaching a steady-state regime, the related nanocatalysts still exhibited better performance than unmodified catalysts.[127,128,131-133]

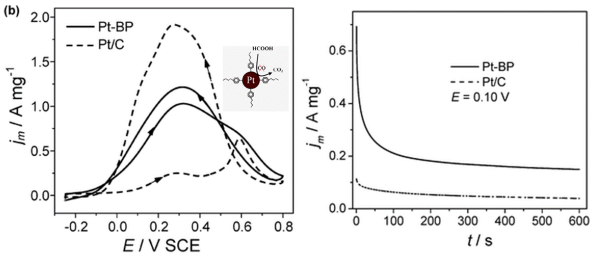

Figure 9. (Left) Cyclic voltammograms at 50 mV s^{-1} and (right) chronoamperometry of Pt-butylphenyl NPs (solid) and Pt/C catalysts (dotted) in 0.1 M H_2SO_4 + 0.1 M HCOOH. Currents were normalized by the mass loading of Pt. Adapted from ref [133] copyright Royal Society of Chemistry 2012

4. Chemical Functionalization of alloys.

Alloying noble metal catalysts with non-noble metals is one effective strategy for enhancing their electrocatalytic activity and concurrently reducing their costs. Initially developed with Pt catalysts to enhance their ORR performance,[104] alloying allows the manipulation of the *d* band center thanks to electronic,[134] and/or geometrical/strain effects,[135] resulting in the tuning of adsorption properties.[136] Such alloying effects can also be combined to metal-ligand interfacial bonding effect. However, there is a limiting number of reports considering this possibility, probably because alloying and metal-ligand interfacial bonding effect have similar purpose. In some reports, alloys are protected by diverse molecules,[137-139] or polymers,[140,141] but without studying their effects on the electrocatalytic performance, even if these stabilizing ligands may have an impact as described in this review. While one work describes a negative effect of ligand coordination on Pt-Ni nanoparticles shaping that leads to lower ORR activity,[142] some examples show the synergy between alloying and metal-ligand interfacial bonding effects for increasing the catalysts' performance.

4.1. Functionalization of alloy nanocatalysts for ORR.

4.1.1. Functionalized Pt alloys.

Many different functionalized nanostructures with different shapes have been described, including Janus nanoparticles,[143,144] nanodendrites,[145] alloys[146,147] and core-shell nanoparticles[148]. Functionalization of PtNi alloys through simple adsorption of cyanide has a positive impact on the onset potential (E_{onset}) and half-wave potential ($E_{1/2}$) of the catalyst compared to commercial Pt black, [149] but especially enhances their methanol tolerance. PtCo nanoparticles have been functionalized by poly(N-isopropylacrylamide) (PNIPAM),[150] improving their catalytic durability (Figure 10). Whereas after accelerated durability test, non-functionalized PtCo nanoparticles show significant degradation of their specific activity (-42%), PNIPAM-PtCo specific activity is mostly maintained (-11%).[150] Lee and coworkers synthesized polyallylamine (PAH) functionalized PdPt core-shell nanodendrites that exhibit high selectivity for ORR.[145] Compared to Pt black, E_{onset} and $E_{1/2}$ are 30 mV more positive, with an area-specific kinetic current density 1.8 times larger. Furthermore, these PHA-functionalized PdPt nanodendrites have excellent ethanol tolerance, in contrast to unfunctionalized PdPt nanoparticles.

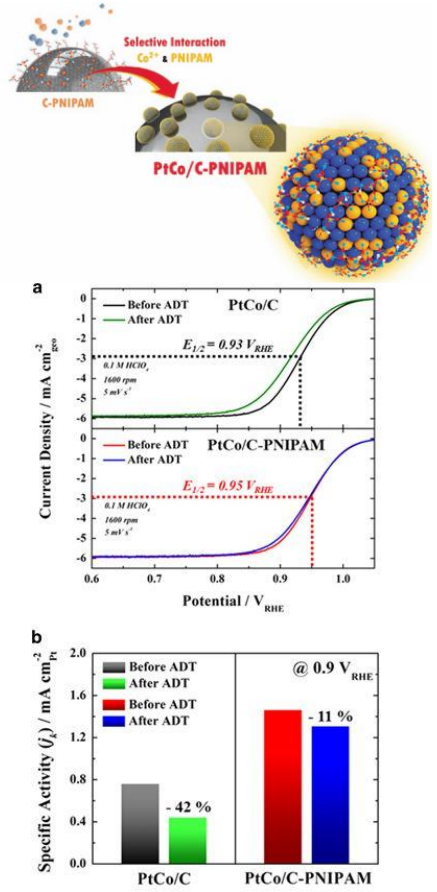

Figure 10. (**top**) Schematic diagram of the surface modification of PtCo nanoparticles using C-PNIPAM. The blue and yellow balls represent the Pt and Co atoms, respectively. (**below**) Electrochemical properties of catalysts before and after accelerated durability test (ADT), showing the high stability of the PNIPAM functionalized particles (a) ORR polarization curves (**b**) the specific activities at 0.9 V_{RHE} for the ORR, From ref [150]. Copyright Nature publishing group 2016.

4.1.2. Functionalized Pd alloys.

Even if alloying Pt decreases its cost and eventually enhances its catalytic performance, other researchers focus their studies on less expensive materials as Pd. Chen *et al*.[147] reported the synthesis and catalytic performance of alkyne-protected AuPd nanoparticles in alkaline media. The best results were obtained with AuPd nanoparticles containing 91.2 at% Pd. Their specific activity is almost doubled and the mass activity is more than eight times that of commercial Pd black, reaching 162 $A.g^{-1}$. Even more importantly, selectivity was enhanced with a number of transferred electrons close to 4, suggesting almost full reduction of oxygen to OH^-. PdNi nanostructures stabilized with polyethyleneimine (PEI) have been reported to exhibits more

positive $E_{1/2}$ and E_{onset} potentials than unfunctionalized PdNi for ORR in acidic media with excellent selectivity.[151] In this case, the number of transferred electrons was 3.9, suggesting an efficient conversion of O_2 to H_2O. These nanocatalysts also show enhanced HER activity compared with PdNi catalysts without PEI. PdNi core-shell nanoparticles stabilized by pyrenebutyric acid were deposited on graphene materials.[148] These materials exhibit improved ORR performance in alkaline media compared to commercial Pd/C, with a 30 mV-more positive E_{onset} potential and a 3.2-fold mass activity increase. The ORR mechanism was suggested to follow a direct four-electron pathway.[148]

4.1.2. Functionalized Ag alloys.

Silver alloys were also studied, although in lesser extent. Chen *et al*. have reported the electrocatalytic activity of AgAu alloy nanoparticles functionalized by 1-dodecyne in alkaline media.[146] The performance of the alloy nanoparticles follows a volcano plot variation with Au content. The best performance is observed for nanoparticles with ca. 35.5 at% Au. These alloy nanomaterials show comparable activity than commercial Pt/C catalysts but outperformed that of pure Ag nanoparticles. Importantly, direct reduction of O_2 to OH^- is obtained with minimal amount of peroxide byproducts, in contrast to hexanethiolate passivated Ag nanoparticles exhibiting a lower *n* value at only 2.5.[143]

4.2. Functionalization of alloy nanocatalysts involved in other fuel molecule reactions.

A small number of examples concerning the activation of other fuel molecules can be found in the literature. Recently, Kauffman and coworkers have reported the electrocatalytic activity of small thiol-capped AuCu nanoparticles toward CO_2RR.[152] When capped with thiols, small (2 nm) bimetallic AuCu (49 at% Cu) nanoparticles convert selectively CO_2 to CO with nearly 100% FE with a cathodic E_{onset} shift of 120 mV. In contrast, nanoparticles synthesized without thiol ligands only produced minor amounts of CO (4% FE) with predominant H_2 evolution. Xu *et al*. have described the strong effect of poly(vinylpyrrolidone) (PVP), poly(vinylalcohol) (PVA) and citrate stabilizers on the catalytic activity of Pt-on-Au (Pt^Au) nanostructures (10 at% Pt) towards FAOR.[110] All stabilized Pt^Au nanostructures show oxidation peak potential lower than 0.6 V vs SCE, suggesting that FAOR proceed through a dehydrogenation mechanism or by the direct reaction pathway.[153] Pt^Au nanostructures stabilized by PVP show enhanced mass-specific activity by 2 to 3 times compared to Pt^Au nanostructures stabilized by PVA and citrates.

5. Influence of organic ligands on surface properties: steric, electronic and interfacial chemical effects

All the different examples described in the above sections demonstrate the impact of surface modification with organic molecules on several electrocatalytic processes. This molecular approach appears now very promising.[154] The effects or the fundamental reasons for such molecular enhancement of electrocatalysis performance are not yet established. First this approach has just recently emerged compared to traditional approaches like the manipulation of size and alloying of metallic catalysts. Second, a wide range of surface modifications procedures could be implemented by involving a large number of possible chemical structures of ligands as well. Hence there are many possible types of interactions between the surface and the organic ligands and between the modified surface and electrolyte. Moreover, it remains very difficult to mitigate the sole effects of organic ligands from others contributing factors such as nanoparticle structure, shape or support. One reason is the difficulty to synthesize the same nanomaterials independently from the capping agents (i.e. with the same shape, size and defects) as comparative models. As a tentative for rationalizing the tuning of the electrocatalytic activity due to organic modifyers, we may distinguish three major effects.

5.1. Steric blocking effect

This aspect refers to a “simple” geometric effect. The ligands occupy some sites, even partially, and hinder the adsorption of other molecules. This may help a reaction for instance by avoiding or limiting poisoning [51,82,94,126-128,130-133,145,149] or by modifying the adsorption affinity of reactants.[54,67,71] This has also strong effect on the durability of the catalysts, by stabilizing the catalyst microstructure or nanostructure. In the context of interfacial chemistry, the steric blocking effect can be met in the literature as “third body effect” or “ensemble effect”.[58,61,82,125] Many multi-step reactions require an active site that consists in a minimum number of adjacent surface atoms, and sometimes in a specific spatial configuration. The active site can thus accommodate simultaneously and/or sequentially the corresponding reactants, intermediates and products, impacting the selectivity and efficiency of the process.

5.2. Electronic structure effect

To avoid/promote adsorption, the effect can be not only geometric but also electronic through metal-ligands interactions. This effect arises from alterations in electronic properties of the metal caused by the chemical functionalization, especially through the formation of strong chemical bonds between the metal surface and ligands, or by structural strain induced by the chemical bonding.[155] The consequence is large changes in the profile of the density of states of valence electrons and therefore in the electron density near the Fermi levels of metals. Let’s recall that the optical or electronic properties of particles can also be manipulated as a result of unique bonding interactions between the metal cores and the organic capping ligands. The ligand-metal interactions may lead to distortions of surface lattice and partial electron transfer that have a direct effect on the adsorption energy of subsequent adsorbate. This effect has been widely put forward to explain the difference in reactivity between naked and modified catalysts as explained in sections 3 and 4.[53,62,65,86,89-93,105,110,120,132,133,150]. This effect has been evidenced in theoretically or experimentally, for instance by employing X-ray absorption fine structure spectroscopy (XAFS), Synchrotron

based photoelectron spectroscopy, X-ray absorption spectroscopy.[91][93]

5.3. Interactions with reactants/intermediates at the catalysts/electrolyte interface

This issue was more scarcely addressed in the reviewed papers than the electronic effect but is probably very interesting to "domesticate" for increasing the performance of catalysts in several directions. This aspect is more related to a chemical effect, by taking benefit of the chemical properties of the organic ligands. Ligands decorating the electrocatalysts could confer specific physicochemical properties, such as high solubility for O_2 or CO_2, [98,118] hydrophilic or hydrophobic properties.[50] They can modulate the interactions between electrolyte and the surface.[72,119] They could modify the orientation of the reactants or intermediate species with respect to the catalytic sites, hence governing selectivity.[59,72,126] The modifications of the surface may enhance the co-adsorption of relevant reactants or intermediates and/or facilitates proton transfers or water activation that are of great importance in these processes.[51,52,60,66,75,127]. They could promote or inhibit certain reaction pathways. Especially, this dimension is very well mastered by Nature for instance in metalloenzymes that catalyze with a rare efficiency many of the processes considered in this review.

All these effects are likely to contribute all together, although probably at different levels according to the nature of the organic ligands, but it is certainly almost impossible to distinguish and to separately exercise fine control on the different contributions.

6. Conclusion

Far to have an adverse impact on the catalytic performance, the presence of organic ligands onto catalytic surface have a beneficial role, although still unpredictable. The exhaustive overview of literature data reported herein shows increasing experimental evidences, validating this approach for activation of small molecules. Importantly, we found that the approach is not limited to a unique process since related works report on ORR, CO_2RR, COR, MOR, FAOR. From a mechanistic point of view, activation of small molecules are usually multi-steps reactions in which adsorption/desorption processes play key roles. In this context, it is reasonable to anticipate strong impact of the presence of ligands on catalytic surfaces. In addition, it is possible to take benefit of the chemical properties of the organic ligands to promote specific interactions toward selective inhibition, as controlled protons relay, or for controlling second coordination sphere interactions with appropriate pendant groups or co-factors. Therefore, in addition to core size and shape control, use of organic ligand agents could bring a complementary strategy for designing efficient, durable and above all, selective catalysts.

A great challenge for taking advantage of the strategy is the rationalized selection of the organic ligands. This includes a good knowledge of the mechanisms of electrocatalytic processes. In addition efforts are required towards the development of comprehensive theory for interpretation of the impact of the surface modification but also experimental characterizations of the physicochemical processes at the metal-ligand interface, notably using *in operando* characterizations.

Acknowledgements

The authors thank J.F. Bergamini for producing the graphical frontispiece.

Keywords: surface modification • electrocatalysis • energy conversion • fuel molecules

[1] Z.-L. Wang, D. Xu, J.-J. Xu, X.-B. Zhang. *Chem. Soc. Rev.* **2014,** *43*, 7746-7786.
[2] F. Cheng, J. Chen. *Chem. Soc. Rev.* **2012,** *41*, 2172-2192.
[3] Y. Kang, P. Yang, N. M. Markovic, V. R. Stamenkovic. *Nano Today* **2016,** *11*, 587-600.
[4] M. Shao, Q. Chang, J.-P. Dodelet, R. Chenitz. *Chem. Rev.* **2016,** *116*, 3594-3657.
[5] J. W. Vickers, D. Alfonso, D. R. Kauffman. *Energy Technol.* **2017,** *5*, 775-795.
[6] J.-H. Zhou, Y.-W. Zhang. *React. Chem. Eng.* **2018,** *3*, 591-625.
[7] Y. Jiao, Y. Zheng, M. Jaroniec, S. Z. Qiao. *Chem. Soc. Rev.* **2015,** *44*, 2060-2086.
[8] M. M. Montemore, M. A. van Spronsen, R. J. Madix, C. M. Friend. *Chem. Rev.* **2018,** *118*, 2816-2862.
[9] H. Mistry, A. S. Varela, S. Kühl, P. Strasser, B. R. Cuenya. *Nature Rev. Mat.* **2016,** *1*, 16009.
[10] M. L. Pegis, C. F. Wise, D. J. Martin, J. M. Mayer. *Chem. Rev.* **2018,** *118*, 2340-2391.
[11] B. Das, A. Thapper, S. Ott, S. B. Colbran. *Sustainable Energy Fuels* **2019,** *3*, 2159-2175.
[12] K. Müller-Dethlefs, P. Hobza. *Chem. Rev.* **2000,** *100*, 143-168.
[13] R. G. Pearson. *J. Am. Chem. Soc.* **1963,** *85*, 3533-3539.
[14] D. Bélanger, J. Pinson. *Chem. Soc. Rev.* **2011,** *40*, 3995-4048.
[15] D.-e. Jiang, B. G. Sumpter, S. Dai. *J. Am. Chem. Soc.* **2006,** *128*, 6030-6031.
[16] L. Laurentius, S. R. Stoyanov, S. Gusarov, A. Kovalenko, R. Du, G. P. Lopinski, M. T. McDermott. *ACS Nano* **2011,** *5*, 4219-4227.
[17] F. Mirkhalaf, J. Paprotny, D. J. Schiffrin. *J. Am. Chem. Soc.* **2006,** *128*, 7400-7401.
[18] L. Troian-Gautier, H. Valkenier, A. Mattiuzzi, I. Jabin, N. V. den Brande, B. V. Mele, J. Hubert, F. Reniers, G. Bruylants, C. Lagrost, Y. Leroux. *Chem. Commun.* **2016,** *52*, 10493-10496.
[19] L. Guo, L. Ma, Y. Zhang, X. Cheng, Y. Xu, J. Wang, E. Wang, Z. Peng. *Langmuir* **2016,** *32*, 11514-11519.
[20] H. Meng, P. K. Shen. *Electrochem. Commun.* **2006,** *8*, 588-594.
[21] N. P. Lebedeva, A. Rodes, J. M. Feliu, M. T. M. Koper, R. A. van Santen. *J. Phys. Chem. B* **2002,** *106*, 9863-9872.
[22] A. Kulkarni, S. Siahrostami, A. Patel, J. K. Nørskov. *Chem. Rev.* **2018,** *118*, 2302-2312.
[23] N. Markovic, H. Gasteiger, P. N. Ross. *J. Electrochem. Soc.* **1997,** *144*, 1591-1597.
[24] A. C. C. Tseung, L. L. Wong. *J. Appl. Electrochem.* **1972,** *2*, 211-215.
[25] J. S. Spendelow, A. Wieckowski. *Phys. Chem. Chem. Phys.* **2007,** *9*, 2654-2675.
[26] E. E. Benson, C. P. Kubiak, A. J. Sathrum, J. M. Smieja. *Chem. Soc. Rev.* **2009,** *38*, 89-99.
[27] J. Zhao, X. Wang, Z. Xu, J. S. C. Loo. *J. Mater. Chem. A* **2014,** *2*, 15228-15233.
[28] H. Yoshio, K. Katsuhei, S. Shin. *Chem. Lett.* **1985,** *14*, 1695-1698.

[29] R. Kortlever, J. Shen, K. J. P. Schouten, F. Calle-Vallejo, M. T. M. Koper. *J. Phys. Chem. Lett.* **2015,** *6*, 4073-4082.
[30] C. H. Lee, M. W. Kanan. *ACS Catal.* **2015,** *5*, 465-469.
[31] Y. Chen, M. W. Kanan. *J. Am. Chem. Soc.* **2012,** *134*, 1986-1989.
[32] Y. Hori, H. Wakebe, T. Tsukamoto, O. Koga. *Electrochim. Acta* **1994,** *39*, 1833-1839.
[33] A. A. Peterson, F. Abild-Pedersen, F. Studt, J. Rossmeisl, J. K. Nørskov. *Energy Environ. Sci.* **2010,** *3*, 1311-1315.
[34] R. P. S. Chaplin, A. A. Wragg. *J. Appl. Electrochem.* **2003,** *33*, 1107-1123.
[35] Z. Yin, G. T. R. Palmore, S. Sun. *Trends in Chemistry* **2019,** *1*, 739-750.
[36] A. Loiudice, P. Lobaccaro, E. A. Kamali, T. Thao, B. H. Huang, J. W. Ager, R. Buonsanti. *Angew. Chem., Int. Ed.* **2016,** *55*, 5789-5792.
[37] D. Raciti, C. Wang. *ACS Energy Lett.* **2018,** *3*, 1545-1556.
[38] W. Ju, A. Bagger, G.-P. Hao, A. S. Varela, I. Sinev, V. Bon, B. Roldan Cuenya, S. Kaskel, J. Rossmeisl, P. Strasser. *Nature Commun.* **2017,** *8*, 944.
[39] J. H. Montoya, A. A. Peterson, J. K. Nørskov. *ChemCatChem* **2013,** *5*, 737-742.
[40] X. Nie, M. R. Esopi, M. J. Janik, A. Asthagiri. *Angew. Chem., Int. Ed.* **2013,** *52*, 2459-2462.
[41] W. Sheng, H. A. Gasteiger, Y. Shao-Horn. *J. Electrochem. Soc.* **2010,** *157*, B1529-B1536.
[42] S. Lu, Z. Zhuang. *Sci. China Mater.* **2016,** *59*, 217-238.
[43] Y. X. Chen, M. Heinen, Z. Jusys, R. J. Behm. *Angew. Chem., Int. Ed.* **2006,** *45*, 981-985.
[44] M. Neurock, M. Janik, A. Wieckowski. *Faraday Discuss.* **2009,** *140*, 363-378.
[45] N. Kakati, J. Maiti, S. H. Lee, S. H. Jee, B. Viswanathan, Y. S. Yoon. *Chem. Rev.* **2014,** *114*, 12397-12429.
[46] A. Ali, P. K. Shen. *J. Mater. Chem. A* **2019,** *7*, 22189-22217.
[47] Y. Tong, X. Yan, J. Liang, S. X. Dou. *Small*, DOI:10.1002/smll.201904126 10.1002/smll.201904126, 1904126.
[48] K. Saikawa, M. Nakamura, N. Hoshi. *Electrochem. Commun.* **2018,** *87*, 5-8.
[49] N. M. Marković, R. R. Adžić, B. D. Cahan, E. B. Yeager. *J. Electroanal. Chem.* **1994,** *377*, 249-259.
[50] A. K. Buckley, M. Lee, T. Cheng, R. V. Kazantsev, D. M. Larson, W. A. Goddard Iii, F. D. Toste, F. M. Toma. *J. Am. Chem. Soc.* **2019,** *141*, 7355-7364.
[51] R. B. Moghaddam, P. G. Pickup. *Electrochim. Acta* **2013,** *107*, 225-230.
[52] S. Zhong, X. Yang, Z. Cao, X. Dong, S. M. Kozlov, L. Falivene, J.-K. Huang, X. Zhou, M. N. Hedhili, Z. Lai, K.-W. Huang, Y. Han, L. Cavallo, L.-J. Li. *Chem. Commun.* **2018,** *54*, 11324-11327.
[53] Z. Cao, J. S. Derrick, J. Xu, R. Gao, M. Gong, E. M. Nichols, P. T. Smith, X. Liu, X. Wen, C. Copéret, C. J. Chang. *Angew. Chem., Int. Ed.* **2018,** *57*, 4981-4985.
[54] K. G. Schmitt, A. A. Gewirth. *J. Phys. Chem. C* **2014,** *118*, 17567-17576.
[55] S. R. Swaminathan, Balaji; Krishnan, Ramya; Dhathathreyan, Kaveriptanam Smaban; Velan, Manickam. *J. Electrochem. Sci. Eng.* **2016,** *6*, 215-223.
[56] J. Tamura, A. Ono, Y. Sugano, C. Huang, H. Nishizawa, S. Mikoshiba. *Phys. Chem. Chem. Phys.* **2015,** *17*, 26072-26078.
[57] M. I. Muglali, A. Erbe, Y. Chen, C. Barth, P. Koelsch, M. Rohwerder. *Electrochim. Acta* **2013,** *90*, 17-26.
[58] B. Genorio, D. Strmcnik, R. Subbaraman, D. Tripkovic, G. Karapetrov, V. R. Stamenkovic, S. Pejovnik, N. M. Marković. *Nature Mat.* **2010,** *9*, 998.
[59] M. Gong, Z. Cao, W. Liu, E. M. Nichols, P. T. Smith, J. S. Derrick, Y.-S. Liu, J. Liu, X. Wen, C. J. Chang. *ACS Cent. Sci.* **2017,** *3*, 1032-1040.
[60] Y. Fang, J. C. Flake. *J. Am. Chem. Soc.* **2017,** *139*, 3399-3405.
[61] B. Genorio, R. Subbaraman, D. Strmcnik, D. Tripkovic, V. R. Stamenkovic, N. M. Markovic. *Angew. Chem., Int. Ed.* **2011,** *50*, 5468-5472.
[62] Z. Cao, S. B. Zacate, X. Sun, J. Liu, E. M. Hale, W. P. Carson, S. B. Tyndall, J. Xu, X. Liu, X. Liu, C. Song, J.-h. Luo, M.-J. Cheng, X. Wen, W. Liu. *Angew. Chem., Int. Ed.* **2018,** *57*, 12675-12679.
[63] Y. Chen, C. W. Li, M. W. Kanan. *J. Am. Chem. Soc.* **2012,** *134*, 19969-19972.
[64] Q. Lu, J. Rosen, Y. Zhou, G. S. Hutchings, Y. C. Kimmel, J. G. Chen, F. Jiao. *Nature Commun.* **2014,** *5*, 3242.
[65] Z. Cao, D. Kim, D. Hong, Y. Yu, J. Xu, S. Lin, X. Wen, E. M. Nichols, K. Jeong, J. A. Reimer, P. Yang, C. J. Chang. *J. Am. Chem. Soc.* **2016,** *138*, 8120-8125.
[66] L. Ma, W. Hu, Q. Pan, L. Zou, Z. Zou, K. Wen, H. Yang. *J. CO2 Utilization* **2019,** *34*, 108-114.
[67] Y. Zhao, C. Wang, Y. Liu, D. R. MacFarlane, G. G. Wallace. *Adv. Energy Mater.* **2018,** *8*, 1801400.
[68] J. A. Trindell, J. Clausmeyer, R. M. Crooks. *J. Am. Chem. Soc.* **2017,** *139*, 16161-16167.
[69] H. Mistry, R. Reske, Z. Zeng, Z.-J. Zhao, J. Greeley, P. Strasser, B. R. Cuenya. *J. Am. Chem. Soc.* **2014,** *136*, 16473-16476.
[70] C. Kim, H. S. Jeon, T. Eom, M. S. Jee, H. Kim, C. M. Friend, B. K. Min, Y. J. Hwang. *J. Am. Chem. Soc.* **2015,** *137*, 13844-13850.
[71] C. Kim, T. Eom, M. S. Jee, H. Jung, H. Kim, B. K. Min, Y. J. Hwang. *ACS Catal.* **2017,** *7*, 779-785.
[72] J. R. Pankhurst, Y. T. Guntern, M. Mensi, R. Buonsanti. *Chem. Sci.* **2019,** *10*, 10356-10365.
[73] M. S. Xie, B. Y. Xia, Y. Li, Y. Yan, Y. Yang, Q. Sun, S. H. Chan, A. Fisher, X. Wang. *Energy Environ. Sci.* **2016,** *9*, 1687-1695.
[74] A. A. Peterson, J. K. Nørskov. *J. Phys. Chem. Lett.* **2012,** *3*, 251-258.
[75] H. Liu, K. Xiang, Y. Liu, F. Zhu, M. Zou, X. Yan, L. Chai. *ChemElectroChem* **2018,** *5*, 3991-3999.
[76] M. Sharma, N. Jung, S. J. Yoo. *Chem. Mat.* **2018,** *30*, 2-24.
[77] J. Gan, W. Luo, W. Chen, J. Guo, Z. Xiang, B. Chen, F. Yang, Y. Cao, F. Song, X. Duan, X. Zhou. *Eur. J. Inorg. Chem.* **2019,** *2019*, 3210-3217.
[78] I. Katsounaros, S. Cherevko, A. R. Zeradjanin, K. J. J. Mayrhofer. *Angew. Chem., Int. Ed.* **2014,** *53*, 102-121.
[79] M. Shao, A. Peles, K. Shoemaker. *Nano Lett.* **2011,** *11*, 3714-3719.
[80] A. Anastasopoulos, J. C. Davies, L. Hannah, B. E. Hayden, C. E. Lee, C. Milhano, C. Mormiche, L. Offin. *ChemSusChem* **2013,** *6*, 1973-1982.
[81] J. E. Newton, J. A. Preece, N. V. Rees, S. L. Horswell. *Phys. Chem. Chem. Phys.* **2014,** *16*, 11435-11446.
[82] Y.-H. Chung, S. J. Kim, D. Y. Chung, H. Y. Park, Y.-E. Sung, S. J. Yoo, J. H. Jang. *Chem. Commun.* **2015,** *51*, 2968-2971.
[83] G.-R. Xu, B. Wang, J.-Y. Zhu, F.-Y. Liu, Y. Chen, J.-H. Zeng, J.-X. Jiang, Z.-H. Liu, Y.-W. Tang, J.-M. Lee. *ACS Catal.* **2016,** *6*, 5260-5267.
[84] G. Fu, K. Wu, X. Jiang, L. Tao, Y. Chen, J. Lin, Y. Zhou, S. Wei, Y. Tang, T. Lu, X. Xia. *Phys. Chem. Chem. Phys.* **2013,** *15*, 3793-3802.
[85] S. Chen, Z. Wei, X. Qi, L. Dong, Y.-G. Guo, L. Wan, Z. Shao, L. Li. *J. Am. Chem. Soc.* **2012,** *134*, 13252-13255.
[86] Z.-Y. Zhou, X. Kang, Y. Song, S. Chen. *J. Phys. Chem. C* **2012,** *116*, 10592-10598.
[87] Z.-Y. Zhou, X. Kang, Y. Song, S. Chen. *Chem. Commun.* **2012,** *48*, 3391-3393.
[88] K. Liu, X. Kang, Z.-Y. Zhou, Y. Song, L. J. Lee, D. Tian, S. Chen. *J. Electroanal. Chem.* **2013,** *688*, 143-150.
[89] C. N. Kostelansky, J. J. Pietron, M.-S. Chen, W. J. Dressick, K. E. Swider-Lyons, D. E. Ramaker, R. M. Stroud, C. A. Klug, B. S. Zelakiewicz, T. L. Schull. *J. Phys. Chem. B* **2006,** *110*, 21487-21496.
[90] J. Pietron, Y. Garsany, O. Baturina. *ECS Trans.* **2007,** *11*, 217-226.
[91] D. S. Gatewood, T. L. Schull, O. Baturina, J. J. Pietron, Y. Garsany, K. E. Swider-Lyons, D. E. Ramaker. *J. Phys. Chem. C* **2008,** *112*, 4961-4970.
[92] J. J. Pietron, Y. Garsany, O. Baturina, K. E. Swider-Lyons, R. M. Stroud, D. E. Ramaker, T. L. Schull. *Electrochem. Solid-State Lett.* **2008,** *11*, B161-B165.
[93] Y.-H. Chung, D. Y. Chung, N. Jung, Y.-E. Sung. *J. Phys. Chem. Lett.* **2013,** *4*, 1304-1309.
[94] N. Jung, H. Shin, M. Kim, I. Jang, H.-J. Kim, J. Hyun Jang, H. Kim, S. Yoo. *Nano Energy* **2015,** *17*.
[95] L. M. Forbes, S. Sattayasamitsathit, P. F. Xu, A. O'Mahony, I. A. Samek, K. Kaufmann, J. Wang, J. N. Cha. *J. Mater. Chem. A* **2013,** *1*, 10267-10273.

[96] P. Hu, L. Chen, C. P. Deming, J.-E. Lu, L. W. Bonny, S. Chen. *Nanoscale* **2016,** *8*, 12013-12021.
[97] K. Miyabayashi, H. Nishihara, M. Miyake. *Langmuir* **2014,** *30*, 2936-2942.
[98] K. Miyabayashi, M. Miyake. *Electroanalysis* **2017,** *29*, 898-906.
[99] P. Joshi, T. Okada, K. Miyabayashi, M. Miyake. *Anal. Chem.* **2018,** *90*, 6116-6123.
[100] S.-i. Yamazaki, M. Asahi, T. Ioroi. *Electrochim. Acta* **2019,** *297*, 725-734.
[101] K. J. J. Mayrhofer, B. B. Blizanac, M. Arenz, V. R. Stamenkovic, P. N. Ross, N. M. Markovic. *J. Phys. Chem. B* **2005,** *109*, 14433-14440.
[102] K. Kinoshita. *J. Electrochem. Soc.* **1990,** *137*, 845-848.
[103] Q. Pang, Y. Zhang, J.-M. Zhang, K.-W. Xu. *Appl. Surf. Sci.* **2011,** *257*, 3047-3054.
[104] J. Greeley, I. E. L. Stephens, A. S. Bondarenko, T. P. Johansson, H. A. Hansen, T. F. Jaramillo, J. Rossmeisl, I. Chorkendorff, J. K. Nørskov. *Nature Chem.* **2009,** *1*, 552.
[105] L. Lu, Z. Wang, S. Zou, Y. Zhou, W. Hong, R. Li, L. Xiao, J. Liu, X.-Q. Gong, J. Fan. *J. Mater. Chem. A* **2018,** *6*, 18884-18890.
[106] G. Fu, X. Jiang, M. Gong, Y. Chen, Y. Tang, J. Lin, T. Lu. *Nanoscale* **2014,** *6*, 8226-8234.
[107] P. Rodriguez, M. T. M. Koper. *Phys. Chem. Chem. Phys.* **2014,** *16*, 13583-13594.
[108] D. Alba-Molina, A. R. Puente Santiago, J. J. Giner-Casares, M. T. Martín-Romero, L. Camacho, R. Luque, M. Cano. *J. Phys. Chem. C* **2019,** *123*, 9807-9812.
[109] W. Chen, S. Chen. *Angew. Chem., Int. Ed.* **2009,** *48*, 4386-4389.
[110] G.-R. Zhang, B.-Q. Xu. *Nanoscale* **2010,** *2*, 2798-2804.
[111] D. Alba-Molina, A. R. Puente Santiago, J. J. Giner-Casares, E. Rodríguez-Castellón, M. T. Martín-Romero, L. Camacho, R. Luque, M. Cano. *J. Mater. Chem. A* **2019,** *7*, 20425-20434.
[112] R. R. Adić, N. M. Marković, V. B. Vešović. *J. Electroanal. Chem. Interfacial Electrochem.* **1984,** *165*, 105-120.
[113] B. B. Blizanac, C. A. Lucas, M. E. Gallagher, M. Arenz, P. N. Ross, N. M. Marković. *J. Phys. Chem. B* **2004,** *108*, 625-634.
[114] R. R. Adžić, S. Strbac, N. Anastasijević. *Mat. Chem. Phys.* **1989,** *22*, 349-375.
[115] Y. Lee, A. Loew, S. Sun. *Chem. Mat.* **2010,** *22*, 755-761.
[116] K. R. Lee, E. S. Kang, Y.-T. Kim, N. H. Kim, D. Youn, Y. D. Kim, J. Lee, Y. H. Kim. *Catal. Today* **2017,** *295*, 95-101.
[117] A. Morozan, S. Donck, V. Artero, E. Gravel, E. Doris. *Nanoscale* **2015,** *7*, 17274-17277.
[118] A. Lanterna, E. Pino, A. Doménech-Carbó, M. González-Béjar, J. Pérez-Prieto. *Nanoscale* **2014,** *6*, 9550-9553.
[119] F. Mirkhalaf, D. J. Schiffrin. *Langmuir* **2010,** *26*, 14995-15001.
[120] L. Lu, S. Zou, Y. Zhou, J. Liu, R. Li, Z. Xu, L. Xiao, J. Fan. *Catal. Sci. Technol.* **2018,** *8*, 746-754.
[121] L. Sumner, N. A. Sakthivel, H. Schrock, K. Artyushkova, A. Dass, S. Chakraborty. *J. Phys. Chem. C* **2018,** *122*, 24809-24817.
[122] J. Guo, J. Zhou, D. Chu, R. Chen. *J. Phys. Chem. C* **2013,** *117*, 4006-4017.
[123] K. Lee, M. S. Ahmed, S. Jeon. *J. Electrochem. Soc.* **2015,** *162*, F1-F8.
[124] K. Liu, Y. Song, S. Chen. *J. Power Sources* **2014,** *268*, 469-475.
[125] S.-W. Yun, S.-A. Park, T.-J. Kim, J.-H. Kim, G.-W. Pak, Y.-T. Kim. *ChemSusChem* **2017,** *10*, 489-493.
[126] T. Wang, Z.-X. Chen, S. Yu, T. Sheng, H.-B. Ma, L.-N. Chen, M. Rauf, H.-P. Xia, Z.-Y. Zhou, S.-G. Sun. *Energy Environ. Sci.* **2018,** *11*, 166-171.
[127] C. Susut, D.-J. Chen, S.-G. Sun, Y. J. Tong. *Phys. Chem. Chem. Phys.* **2011,** *13*, 7467-7474.
[128] X. Gao, Y. Li, Q. Zhang, S. Li, Y. Chen, J.-M. Lee. *J. Mater. Chem. A* **2015,** *3*, 12000-12004.
[129] M. Cao, D. Wu, S. Gao, R. Cao. *Chem. Eur. J.* **2012,** *18*, 12978-12985.
[130] Y. Guo, Y. Wu, R. Cao, S. Zheng, Y. Yang, M. Chen. *J. Electroanal. Chem.* **2017,** *785*, 159-165.
[131] Y. Yıldız, S. Kuzu, B. Sen, A. Savk, S. Akocak, F. Şen. *Int. J. Hydrogen Energy* **2017,** *42*, 13061-13069.
[132] Z.-Y. Zhou, X. Kang, Y. Song, S. Chen. *Chem. Commun.* **2011,** *47*, 6075-6077.
[133] Z.-Y. Zhou, J. Ren, X. Kang, Y. Song, S.-G. Sun, S. Chen. *Phys. Chem. Chem. Phys.* **2012,** *14*, 1412-1417.
[134] Y. Gauthier, M. Schmid, S. Padovani, E. Lundgren, V. Buš, G. Kresse, J. Redinger, P. Varga. *Phys. Rev. Lett.* **2001,** *87*, 036103.
[135] M. Mavrikakis, B. Hammer, J. K. Nørskov. *Phys. Rev. Lett.* **1998,** *81*, 2819-2822.
[136] J. R. Kitchin, J. K. Nørskov, M. A. Barteau, J. G. Chen. *J. Chem. Phys.* **2004,** *120*, 10240-10246.
[137] Ö. Metin, X. Sun, S. Sun. *Nanoscale* **2013,** *5*, 910-912.
[138] D. Kim, J. Resasco, Y. Yu, A. M. Asiri, P. Yang. *Nature Commun.* **2014,** *5*, 4948.
[139] Y. Chen, Z. Liang, F. Yang, Y. Liu, S. Chen. *J. Phys. Chem. C* **2011,** *115*, 24073-24079.
[140] Y. Lu, Y. Jiang, W. Chen. *Nano Energy* **2013,** *2*, 836-844.
[141] Q. Shi, C. Zhu, C. Bi, H. Xia, M. H. Engelhard, D. Du, Y. Lin. *J. Mater. Chem. A* **2017,** *5*, 23952-23959.
[142] F. Qin, Y. Ma, L. Miao, Z. Wang, L. Gan. *ACS Omega* **2019,** *4*, 8305-8311.
[143] Y. Song, K. Liu, S. Chen. *Langmuir* **2012,** *28*, 17143-17152.
[144] L. Chen, C. P. Deming, Y. Peng, P. Hu, J. Stofan, S. Chen. *Nanoscale* **2016,** *8*, 14565-14572.
[145] F.-M. Li, X.-Q. Gao, S.-N. Li, Y. Chen, J.-M. Lee. *NPG Asia Mater.* **2015,** *7*, e219-e219.
[146] P. Hu, Y. Song, L. Chen, S. Chen. *Nanoscale* **2015,** *7*, 9627-9636.
[147] C. P. Deming, A. Zhao, Y. Song, K. Liu, M. M. Khan, V. M. Yates, S. Chen. *ChemElectroChem* **2015,** *2*, 1719-1727.
[148] D. K. Perivoliotis, Y. Sato, K. Suenaga, N. Tagmatarchis. *Chem. Eur. J.* **2019,** *25*, 11105-11113.
[149] H. Liu, X. Liu, Y. Li, Y. Jia, Y. Tang, Y. Chen. *Nano res.* **2016,** *9*, 3494-3503.
[150] N. Jung, S. Bhattacharjee, S. Gautam, H.-Y. Park, J. Ryu, Y.-H. Chung, S.-Y. Lee, I. Jang, J. H. Jang, S. H. Park, D. Y. Chung, Y.-E. Sung, K.-H. Chae, U. V. Waghmare, S.-C. Lee, S. J. Yoo. *NPG Asia Mater.* **2016,** *8*, e237-e237.
[151] Y. Zhao, Y. Ding, B. Qiao, K. Zheng, P. Liu, F. Li, S. Li, Y. Chen. *J. Mater. Chem. A* **2018,** *6*, 17771-17777.
[152] D. R. Kauffman, D. R. Alfonso, D. N. Tafen, C. Wang, Y. Zhou, Y. Yu, J. W. Lekse, X. Deng, V. Espinoza, J. Trindell, O. K. Ranasingha, A. Roy, J.-S. Lee, H. L. Xin. *J. Phys. Chem. C* **2018,** *122*, 27991-28000.
[153] D. Zhao, Y.-H. Wang, B.-Q. Xu. *J. Phys. Chem. C* **2009,** *113*, 20903-20911.
[154] D.-H. Nam, P. De Luna, A. Rosas-Hernández, A. Thevenon, F. Li, T. Agapie, J. C. Peters, O. Shekhah, M. Eddaoudi, E. H. Sargent. *Nature Mat.* **2020,** *19*, 266-276.
[155] P. Hu, L. Chen, X. Kang, S. Chen. *Acc. Chem. Res.* **2016,** *49*, 2251-2260.

Entry for the Table of Contents

REVIEW

A tale of synergy between organic ligands and metallic catalysts

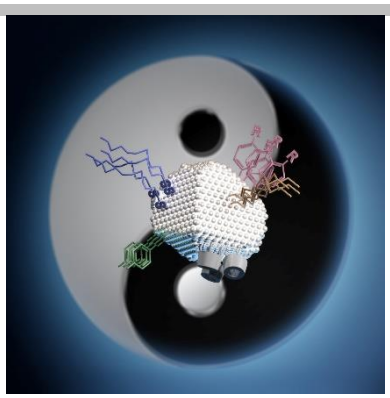

*Quentin Lenne, Yann Leroux, Corinne Lagrost**

Page No. – Page No.

Surface modification for promoting durable, efficient and selective electrocatalysts